Master's thesis

NTNU
Norwegian University of Science and Technology
Faculty of Engineering
Department of Manufacturing and Civil Engineering

James Joseph Asirvatham Wesley

Investigating the effect of accelerated aging on the mechanical properties of HDPE used in Norwegian fish farms

Master's thesis in Sustainable Manufacturing

Supervisor: Dr. Sotirios Grammatikos

November 2020

NTNU
Norwegian University of Science and Technology

James Joseph Asirvatham Wesley

Investigating the effect of accelerated aging on the mechanical properties of HDPE used in Norwegian fish farms

Master's thesis in Sustainable Manufacturing
Supervisor: Dr. Sotirios Grammatikos
November 2020

Norwegian University of Science and Technology
Faculty of Engineering
Department of Manufacturing and Civil Engineering

NTNU
Norwegian University of
Science and Technology

Abstract

The goal of this study is to analyse the properties of High-Density Polyethylene (HDPE) used in fish farms when subjected to various environmental factors such as sunlight, rain, moisture, and humidity experienced in the Norwegian coastline. The investigation is done by simulating the natural aging process by means of artificial weathering in UV chambers. The HDPE is fabricated by means of Injection moulding, subjected to different aging periods, tested, at various intervals to determine the degradation of mechanical properties at selected aging intervals. The degradation in mechanical properties is correlated with Hyperspectral imaging to potentially determine polymeric degradation/changes without destructive testing. This data will serve as a robust base for the prediction of the lifetime of HDPE used in an aquatic environment.

Acknowledgements

The research work done so far was performed in collaboration with SINTEF Raufoss Manufacturing, within Plasto's MEGAMOULD project. The work done in this study will be used by Plasto to enhance their work done for Norwegian fish farms. I would like to thank my supervisor Dr. Sotirios Grammatikos for the opportunity to work on this project, his guidance and expert advice on polymer degradation, materials and aging, PhD student Chaman Srivastava for always taking time to offer guidance, motivation, sharing his knowledge, and helping with interpreting the testing results. I would like to thank lab engineer Pal Erik Endrerud for sharing his expertise and assisting in setting up and conducting the accelerated aging, maintenance and calibration of equipment and being available whenever there was a technical difficulty.

Also, I would like to thank my friends on and off campus for keeping me on track and the motivation to keep me focussed.

Gjovik, 6th November 2020

James Asirvatham

Table of contents

List of figures

Acronyms

HDPE	High Density Polyethylene
LDPE	Low density Polyethylene
HSI	Hyperspectral Imaging
UV	Ultraviolet
RMSE	Root Mean-Square Error
PE	Polyethylene
UTS	Ultimate Tensile Strength
LTS	Lower Tensile Stress

1.Introduction

The global demand for marine protein has increased over the years and aquaculture has been employed to match this growing demand. Aquaculture is the culture of aquatic plants and animals under semi controlled or fully controlled conditions. In the broadest sense, aquaculture is essentially underwater agriculture(Tidwell and Bright, 2019). Aquaculture utilises artificial enclosure and equipment to breed marine-life for consumption and is viewed as a sustainable method to produce marine protein(Feng et al., 2019). Man started off as a hunter gatherer and slowly moved into farming and domestication. There was a larger focus on land-based cultivation until the advent of Aquaculture. Aquaculture is currently the world's fastest growing food production sector and it possesses excellent characteristics that enable it to be one of the most efficient and low environmental impact methods of producing high quality protein for the human population(Ojha and Babu, 2019). Aquaculture as an industry is growing rapidly across the globe. According to the FAO, between 1985 to 2016, the percentage of finfish farmed using aquaculture in terms of grew from 19% to 44% (FAO ,2016). FAO has reported that in terms of global volume of production, farmed fish exceeded capture fisheries in 2013. FAO regards aquaculture as a promising solution to the food crisis that exists in the world and a reliable source of protein for the growing masses.

Norway is a country defined by the sea, rooted in over thousand years of fishing. With nearly 101,000 kilometres of combined mainland and island coastline, Norway has a powerful connection with the sea. The Norwegian aquaculture sector has capitalized on their favourable and rugged geography which includes deep fjords and immaculate ocean water as well as the Gulf stream providing a reliable and stable temperature, has been proven to provide excellent opportunities for this kind of intensive fish farming. Norway's quest with aquaculture dates to 1850, when brown trout was successfully hatched, followed by a commercial breakthrough in the early 1960s and it has grown exponentially since then. Most of the growth occurred between 2000 and 2016. The growth has been supported and augmented by governmental support and the industrial support to ensure sustainable production. The main species that is farmed in Norway is Atlantic Salmon, which makes 93% of Norway's aquaculture, this is followed by Rainbow Trout, Mussels

and Atlantic Halibut. Other species farmed include Atlantic Cod and Artic Char. Export accounts for almost 95% of the Norwegian aquaculture production which makes its way into more than 130 different countries.

Industries of today are scrambling to find sustainable solutions to feed growing populations. Aquaculture presents itself as a promising solution to meet the world's demand for seafood. It is a very sustainable means of production as the rate at which the fish stock replenishes is greater that the demand of the market. Currently, 17% of global protein consumption comes from the sea, and it is predicted to grow up to 40% by 2050 at the current rate of growth. In 2014 aquaculture exceeded fisheries production by 10 million metric tons and FAO estimates that by 2030, two thirds of all seafood consumed would be farmed. Plastics are versatile and cost-effective substances that have enabled human flourishing across all areas of life, ranging from aerospace applications, food packaging to high fidelity hospital use that has proved to be lifesaving. Due to the ideal properties of plastics such as low density, high strength, resistance to corrosion and user-friendly design, plastic usage has become exceeded the usage of aluminium and other metals(Devasahayam et al., 2019). Hence, aquaculture as an industry have employed plastics as an integral material in their process and production activities Many of these polymeric materials used in aquaculture have proven to be cost-effective and have enhanced efficiency and productivity(AKVAGroup, 2018). In particular, the Norwegian aquaculture industry has grown exponential since its inception in the 1970s. Norway produced over 65% of the world's Atlantic salmon in 2019. Today, fish farming is thriving along the Norwegian coastline, producing an excess of over 1,2 million tonnes per year, out of which 95% is exported. (Dyrevernalliansen, 2016). Plastics are instrumental and have become increasingly important materials in fish farms as most of the equipment used in aquaculture, such as nets, pens, and buoys. Over the years, fish farms have moved further into the sea and thus the fish farm equipment experience harsher environmental conditions and greater fatigue. The environmental factors are not the only threat at sea. The presence of predatory marine organisms is a growing problem as well. Most of the plastic loss in fish farms were due to extreme weather, installation wear, poor waste management and erratic maintenance(ASC, 2018). HDPE is a polyolefin that is of great commercial and economic importance. It is an attractive material for testing and analysis due to its versatility, low cost, and excellent properties. In 1974, the AKVA group launched the first circular plastic cage, Polarcirkel. It has a modular construction; hence it is mobile and extensible and constructed using HDPE. The structure along with the choice of material results in an environment that is conducive to aquaculture, with

improved fish mobility, low toxicity and microplastic concentration, increased oxygenation, and waste removal(AKVAGroup, 2018). HDPE has several properties that make it ideal as a packaging and manufacturing product. It is stronger than standard polyethylene, acts as an effective barrier against moisture and remains solid at room temperature. It resists insects, rot, and other chemicals. It is easily recyclable and can be used repeatedly and does not leak toxic chemicals into soil or water(PE100, 2016). Though HDPE has been beneficial in fish farming, they pose an impending threat due to their accumulation in aquatic systems and the potential waste disposal problems that are associated with degradation. Assessing the degradation of marine-use plastics is hastened by the need to close material loops to preserve our diminishing natural resources when striving towards circular economy(Baran et al., 2016), but also by the concern raised by the accumulation of existing plastic waste in oceans and lakes and the threat posed to marine life at large.

It is therefore of great importance to study the degradation of HDPE, to understand the lifetime of the polymer in a marine environment. The material under study was HDPE, which was supplied by SINTEF Raufoss Manufacturing (SRM), through Plasto. The dog-bone samples were fabricated from the same material used in Norwegian fish farms to ensure testing accuracy. The choice of tests utilised to determine material properties are carefully selected from literature, as they are the most relevant to the fish-farming scenario. HDPE's exposure to UV light and moisture in the QUV chamber would simulate the conditions of sunlight, rain, and moisture. This creates an environment for accelerated aging to occur(Dupuis et al., 2017). QUV testers is to obtain different scenarios of weathering .(Lu et al., 2018), (Tanyildizi, 2018). The tensile testing investigates a major chunk of the HDPE's mechanical properties such as tensile strength, young's modulus, ultimate strength etc(Niemsakul et al., 2018). The flexural tests corroborate the results obtained from the tensile testing and the various mechanical properties are assessed across the aging time to get a better understanding of the effect of aging on the polymer. The hyperspectral imaging is done to study spectral changes in the material and corroborate the findings with rends in the mechanical properties. This is followed by a discussion that builds a case for the results obtained and other observed phenomena, followed by concluding remarks and recommendations/ plans for future work.

2.Theoretical background

This chapter introduces polymers, plastics and uses along with introducing the characterisation techniques along with mechanical testing parameters and theory about the other methods employed in this study. This is to allow for the better interpretation of the methods used and the results obtained.

2.1 Polymers

The word polymer is derived from Greek, poly means many and meros meaning parts(Ram, 1997).A polymer consists of very large molecules made up of many smaller units called monomers which are joined to form a long chain by the process of polymerization. Monomers are called the building blocks of polymers; monomers constitute mostly hydrogen and carbon. Sometimes other elements such as oxygen, nitrogen, chlorine, or fluorine is added to monomers to create different properties and grades of polymers. Multiple monomers together form macromolecules that comprise large molecular chain networks held together by covalent bonds between the atoms. These molecular chains are bonded to each other by forces such as Van der Waals, dipole or hydrogen bonds and sometimes covalent bonds. This cross-linking creates a molecular network resulting in polymers(Roesler et al., 2007). Based on the cross-linking, polymers can be divided into three types: Elastomers, thermoplastics and duromers. I.e: A thermoplastic has no crosslinking, elastomers (rubbers) have a minimal number of crosslinks and duromers (thermosetting polymers) have a large number of crosslinks(Polanco-Loria et al., 2010).

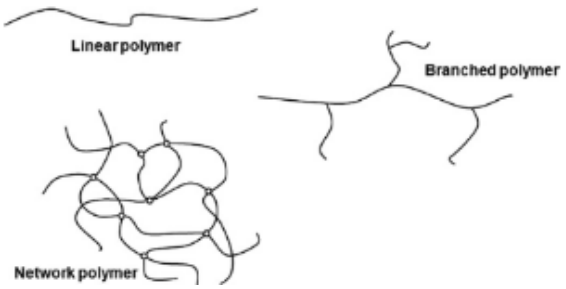

Figure 2.1: Sketch of Polymer types (Rösler et al., 2007)

Table 2.1 Physical and mechanical properties of polymers (Callister, 2007)

Property	Description
Tensile elongation	A measure of how much the material length increases in response to a tensile load. Elongation at break is the maximum elongation the polymer can undergo.
Flexural stiffness	The maximum bending load a material can withstand before it ruptures.
Tensile strength	The maximum tensile load per unit area a material can withstand.
Fatigue	Material deformation and/or failure under a cyclically applied load (tension, compression, or flexure) over time.
Hardness	The resistance to deformation due to surface indentation or abrasion.
Ductility	A measure how well a material can deform without fracture and can be evaluated via tensile elongation.
Brittleness	The opposite to ductility; the tendency of the material to fracture under the application of load without or with small previous deformation.
Viscosity	The resistance of polymer to flow in a molten state by the shear forces. It is indirectly proportional to the Melt Flow Rate
Toughness	The ability to absorb mechanical energy without fracturing. It is proportional to the impact strength.
Impact strength	Evaluates how well the material absorbs energy from an impact loading. In the case of testing a notched sample, it is related to the ease of crack propagation.

2.2 Plastics

The word plastic is derived from the Greek word **πλαστικός** (plastikos) meaning "having the capacity to be shaped or moulded" The plasticity, or malleability, of the material during processing and manufacture allows it to be pressed, cast or extruded into a variety of shapes, such as: films, fibers, plates, tubes, bottles, boxes, amongst many others.The IUPAC definition of plastic is “Generic term used in the case of polymeric material that may contain other substances to improve performance or reduce costs”(Vert et al., 2012)

Though plastics have been around for almost a century and though they have been beneficial across various sectors, and they are broadly clasified into thermoplastics, thermosets and elastomers(Eyerer, 2010).

2.2.1 Thermoplastics:

Thermoplastics are defined as the polymers that can be melted and recast almost infintely. They soften/melt upon heating and harden upon cooling. Thermoplastics have a simple molecular structure and chemically independent macromolecules, this allows for multiple cycles of heating, cooling, processing and recycling(PlasticsEurope, 2016).

2.2.2 Anisotropy:

Thermoplastics are anisotropic, in that their properties vary depending on the direction that they are being measured. There are several reasons for this; one is due to the distribution of polymer molecules throughout the materials, either randomly or organized(Callister, 2007). Two, the processing involved in the manufacture of the thermoplastic. Some processed result in the alignment of the polymer molecules in a certain direction, thereby the properties along the alignment would be different to the ones across the direction of alignment. In some cases, they are determinantal and some cases the resulting properties are intentional to improve properties in a direction. Hence it is importance to study the effect of force in different directions to better understand the structure, mechanical behaviour, and the degradation of the material(Peacock, 2000).

2.2.3 Effect of manufacturing process

The method used to process a polymer has impact on the final properties of it. The mechanical properties of a thermoplastic can differ in different directions based on the processing methods and conditions due to the arrangements/ molecular arrangements along the moulding direction(Amjadi and Fatemi, 2020) if the thermoplastics are processed using injection moulding.

2.3 Polymer degradation

Materials, especially polymers can lose their properties in aging environments(Platzer, 1986). The choice of a polymer for an application is determined by the environment it is used in. weathering agents present such as rain, humidity, pollutants, temperatures, thermal cycles, sunlight, and oxygen. These factors vary from region to region. It is crucial to know the durability of a polymer to evaluate its service life and to enhance its maintenance. The extent of degradation of the polymer, depends on its nature and its interaction with the surrounding environments. The speed at which these changes occur, and the type of changes must take into consideration the variations of mechanical, dielectric, viscoelastic, thermal properties etc. Lack of durability and degradation can impose safety risk and health hazards, even to the point of material failure. The susceptibility of a polymer to degradation depends primarily on its structure. Epoxies and aromatic chains are sensitive to degradation by UV degradation whereas hydrocarbon-based polymers are susceptible to thermal degradation. Polymer components and equipment fail either by bad materials or erroneous engineering design or a combination of both(Scott, 1999)

Weathering plays a huge role in polymer degradation, by means of molecular weight degradation. Constant exposure to weathering elements results in crystallinity causing brittle surface layers like that formed by oxidation(Qiao et al., 2009).

2.3.1 Degradation due to UV

Certain UV wavelengths cause damage to certain polymeric materials. The most damaging region of wavelengths is between 280nm and 315nm(Torikai et al., 1995). The UV degradation is due to the combined effect of photolysis and oxidative reactions(Grigoriadou et al., 2011). The photons which are absorbed excite the electrons and cause bond dissociation. An instance of this is photo decomposition of hydroperoxide groups introduced during melt processing(Szabo, 2005).

$$\mathbf{ROOH} + \boldsymbol{h\nu} \rightarrow \boldsymbol{RO^*} + \boldsymbol{OH^*}$$

A high absorption coefficient indicates that the light penetrates the polymer to a certain depth. However, the intensity drops exponentially with penetration according to the equation

$$\boldsymbol{I} = \boldsymbol{I_0}\mathbf{exp}\,(-\frac{\boldsymbol{x}}{\boldsymbol{L}})$$

i.e. for virgin unpigmented HDPE that is irradiated at a wavelength of 310 nm, which corresponds to a depth of (L=1.25mm)

Since HDPE has high oxidation resistance, it is preferred over other polymers to be used in an oxygen rich environment. Oxygen has a negative impact on polymer properties and is further accelerated by sunlight (photo-oxidation). This compounded effect causes the polymer to become brittle and degrades the mechanical properties.

Photooxidation of polyethylene proceeds by a free radical chain mechanism(Chemtec, 2015). There are four steps involved in this: initiation, propagation, chain branching, and termination. Initiation of this degradation is caused by either the presence of initiator or with the presence of hydroperoxide

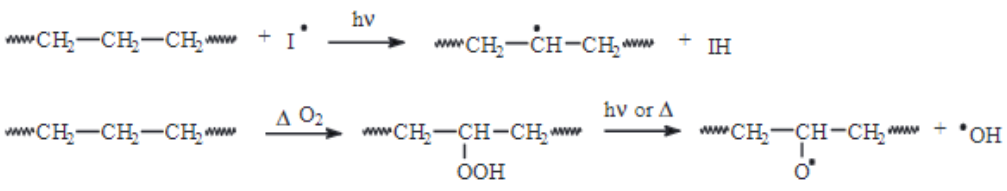

(2.1)

The decomposition of hydroperoxides results in the formation of other radicals due to chain scissions and sometimes cross-linking forming polyethylene unsaturations as depicted below:

(2.2)

The presence of these unsaturations leads to the formation of allylic hydroperoxides during the degradation and forms the major mechanism of initiation such as follows:

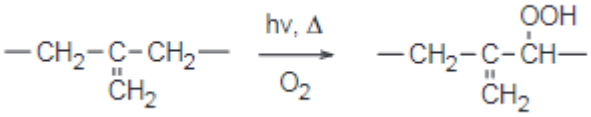

(2.3)

This structure is then converted by UV, heat into freed radical/structures containing the UV-absorbing groups (carbonyl), with chain scission being the dominant reaction(Chemtec, 2015).

A combination of several factors along with UV exposure, such as mechanical stress, temperature, chemical influences etc cause the degradation of the polyethylene.

2.4 Microplastics:

Microplastics are a novel threat to marine ecosystems and is still difficult to define what it really is(Frias and Nash, 2019). Microplastics refer to the particles that arise from the degradation of plastic objects that are present in a marine environment and they are present in different sizes(Van Cauwenberghe et al., 2015). The degradation can occur due to UV radiation, physical abrasion, and moisture and cause them to disperse into a marine environment(Cole et al., 2011). A common consensus on the size is that any plastic fragment less than 5mm is accepted as a microplastic(Cole et al., 2011).

2.4.1 The problem of microplastics

The major issue with microplastics is the ingestion by marine organisms. It has been proven that a variety of diverse marine life across food chains and trophic levels ingest microplastics. A study by (Andrady, 2011) has shown that microplastics accumulate and even end up in human tissue. The plastic could accumulate, permeate into tissue, leach chemicals, or even introduce toxins through cohesion. It is vital to keep in mind that the indirect effect of microplastics is far greater than the direct effect, the largest concern being bioaccumulation. When the microplastics act as a vector for toxins, it acts on the lowest rung of the food chain. Even though the direct effect of the plastic may not be fatal to the lowest rung, the species in higher levels of the food chain would be adversely affected. When marine organisms ingest these microplastics and plastic debris, it accumulates in the food web and gets biomagnified and poses a threat to aquatic life and marine toxicity(IUCN, 2018). In summation, the size of the microplastics results in it negatively affecting the very base of the food chain. Also, the properties of the material itself, result in it attracting toxins. The combination of the two makes microplastic a vector of dangerous, and often unnatural, substances in the marine environment. The vector hits the very core of many marine ecosystems and pose a danger to several organisms, either directly or indirectly. There have been several cases where marine plastics have degraded into smaller particle sizes and it has been a threat to marine life. One such example is HDPE microplastics impairing the development and swimming activity of a pacific oyster larvae, *Crassostrea gigas*. The study by (Bringer et al., 2020) investigates the effects of effect of a 24 hour exposure to HDPE microplastics at different particle sizes (4–6, 11–13 and 20–25 µm) on the development and locomotion of the pacific oyster larvae, Crassostrea gigas. The results show that the smaller microplastics induced greater rates of malformation and developmental arrests than larger ones. All three sizes resulted in a malfunction in straight line swimming. Thus, the presence of microplastics in a marine environment would prove detrimental to the swimming behaviour, survival, and colonization of new habitats for marine species.

2.5 Polyethylene

The simplest thermoplastic polymer is polyethylene (PE). The PE macromolecule is built up by many ethylene monomers. The number of monomers that are joined to form a molecule are around 10^4 but it may vary from 10^3 to 10^6. Owing to the regular chain structure, PE can be easily arranged into crystals and is hence regarded as a semi-crystalline material. Polyethylene has a melting point of 115–130 ◦C and a density of 0.91–0.96 g/cm3. It is based on the density; polyethylene is broadly classified into HDPE and LDPE. A variety of different PE grades can be produced by either chain branching or taking advantage of the strong covalent bonds by highly oriented fibre stretching. The most common forms are low-density polyethylene (LDPE) and high-density polyethylene (HDPE). The difference in density shows that molecular packaging is denser, with a higher crystallinity in HDPE than in LDPE. Depending on the molecular structure, application of PE varies from plastic bags (LDPE) to high performance fishing lines and fish farm equipment (HDPE).

High-density polyethylene (HDPE) is a thermoplastic produced from the monomer ethylene. HDPE is mostly straight chain molecules, and it is tightly packed. In 2007, HDPE production reached a total of more than 30 tons(Ceresana, 2019). Most of HDPE produced is used in the packaging industry (around 48% in 2018)

2.5.1 Molecular structure of Polyethylene

Polyethylene is made by subjecting ethylene gas to the polymerization process, it was first synthesized in England by the Imperial chemical industries in 1933 and has evolved ever since into the commercial thermoplastic we know today.

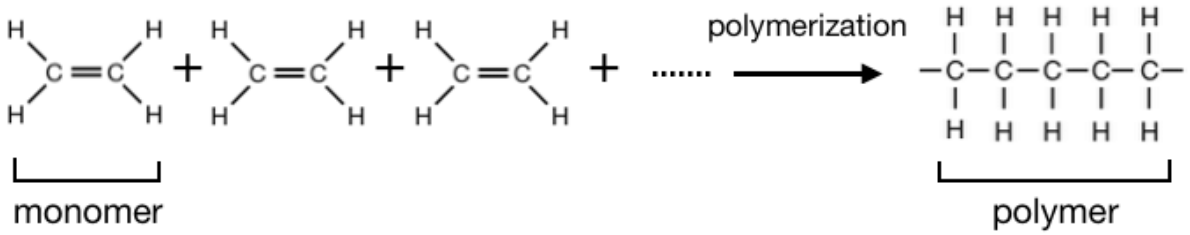

Figure 2.2 : Polymerization of Polyethylene (Demirbay, 2017)

The polyethylene chains have different lengths and are three dimensional, varying from a few hundred to several thousand ethylene units. Further, they can be additionally branched or with little or no branching. The length of the main chain and the side branching is controlled by the polymerization process and influences the molecular weight and the molecular weight distribution of Polyethylene. The polyethylene chains are very randomly organized in the molten, causing the longer chains to entangle. Whereas, when the polymer crystallizes, the PE chains organize themselves in an ordered fashion. Polyethylene is semi-crystalline and consists of a mixture of amorphous and crystalline regions and the final crystallinity of the polymer is determined by the quantity of these regions(Peacock, 2000).

2.5.2 Effect of molecular structure on the mechanical properties of PE:

High molecular weight holds the crystallites together and allows for the transfer of forces between them. In the case of high molecular weight there are interlamellar connections (tie chains) which result in a higher physical strength(Peterlin, 1967). When a load is applied on the material, the tie chains increase the polymer mobility, allowing for a greater elongation. However, due to aging the polymer mobility decreases resulting in lesser elongation, more brittleness and increasing tensile strength(Nicholson et al., 2000). Higher molecular weight increases the polymer durability, long time strength and the fatigue, however the viscosity of the polymer increases, and the melt flow rate is reduced, which is a challenge during polymer processing(Callister, 2007), in this case, injection moulding.

2.5.3 Deformation of polyethylene:

There are several factors that govern the behaviour of polyethylene such as stress mode, magnitude, and the speed of the applied load. It involves the reorganisation of molecules and morphological changes. There are two major modes the deformation proceeds in, which is the ductile mode which involves plastic deformation and the brittle mode which involves a rapid fracture. The deformation and the failure of the specimen is defined by certain parameters such as rate of deformation, temperature, density, crystallinity, the presence of notches and defects etc(Callister, 2007).

One of the most investigated stress modes for polyethylene is tension, which reflects a lot on the material properties and the mechanism of deformation. The stress strain curve

that is obtained post testing depicts the nature of the deformation process. Within the elastic region, the deformation is homogenous and elastic. The elastic modulus is proportional to the crystallinity as more stress is required to elongate the material with the less amorphous regions(Peacock, 2000). The yield point is the first maximum value on the curve, which is followed by necking (plastic deformation). The yield stress increases with the increase in crystallinity. This is followed by cold drawing and strain hardening.

To understand the effect of aging better, the force-elongation curve is divided into the 3 major regions(Xu et al., 2016):

- Elastic: 1st region
- Necking: 2nd region
- Strain hardening and fracture: 3rd region

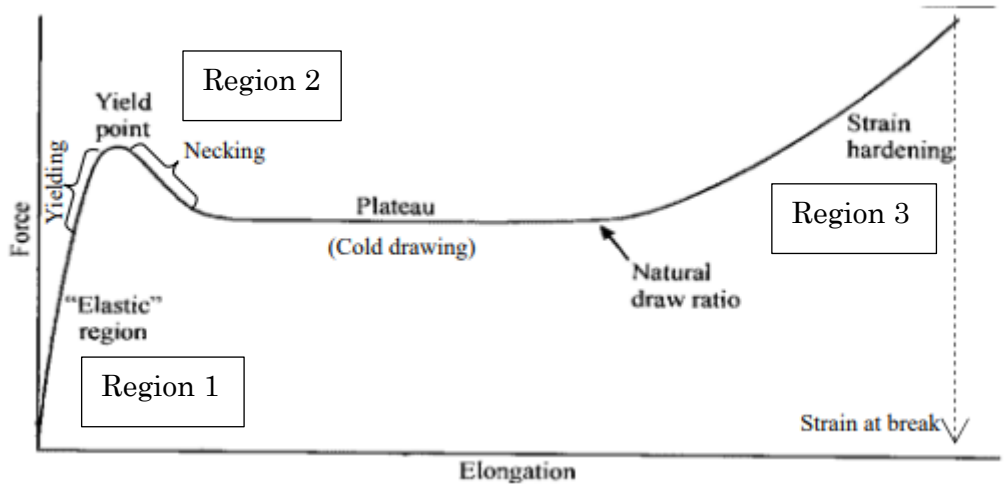

Figure 2.3: Force vs Elongation curve of PE with key stages (Peacock, 2000) (Xu et al., 2016)

2.5.4 Fracture of Polyethylene:

The fracture of polyethylene proceeds with perpendicularly to the direction of the applied stress. The fracture of PE usually involves energy absorption, inelastic deformation, and the formation of a new surface area., The fracture can be in the ductile or brittle mode. A ductile fracture proceeds by crack formation, followed by crazing and yielding prior to fracture. The crazes lead to the formation of micro voids connected by fibrillar bridges moving to chain orientation. When the micro voids grow and coalesce together, they turn into cracks which lead to the ultimate failure of Polyethylene. Ductile fracture results in

a more fibrous surface, whereas brittle fracture results in a flat fracture surface(Peacock, 2000).

2.5.5 Properties of HDPE

HDPE is a strong polymer with one of the highest strength-to-density ratios amongst polymers(Salih et al., 2013). Since HDPE has very little branching, it results in stronger intermolecular forces and greater tensile strength than LDPE(Shebani et al., 2018). Higher molecular weights result in increased tensile strength, higher impact resistance and abrasion resistance. It can withstand high temperatures for short periods of time and is resilient toward different solvents. Since HDPE has a greater rigidity than LDPE, it is optimal for structural applications(Kutz, 2017). Most HDPE's possess an average molecular weight of $50 \times 10^3 - 250 \times 10^3$kg/mol. Special types of HDPE are produced by polymerization reactions.

Table 2.2 : The various properties of HDPE(Sahu and Sudhakar, 2019)

Properties	**Values**
Density (g/cm³)	0.941–0.965
Flexural modulus (MPa)	350–1551
Tensile modulus (MPa)	413–1034
Tensile yield stress (MPa)	18–31
Tensile strength at break (MPa)	22–31
Tensile elongation at break (%)	20–130
Degree of crystallinity (%)	80–95

2.6 Accelerated aging:

Accelerated aging or Accelerated weathering is a type of testing that utilises heat, humidity, sunlight, mechanical vibration etc to speed up the normal aging of materials. It is a useful tool in determining the lifetime of a product/material before the material is used, hence serving as a benchmark to ascertain shelf life/product life(Cysne Barbosa et al., 2017). Accelerated aging is done using an accelerated aging chamber/ environmental aging chamber which creates several combinations of environmental elements as desired(Cysne Barbosa et al., 2017).

2.6.1 Weather conditions in Hjelmeland:

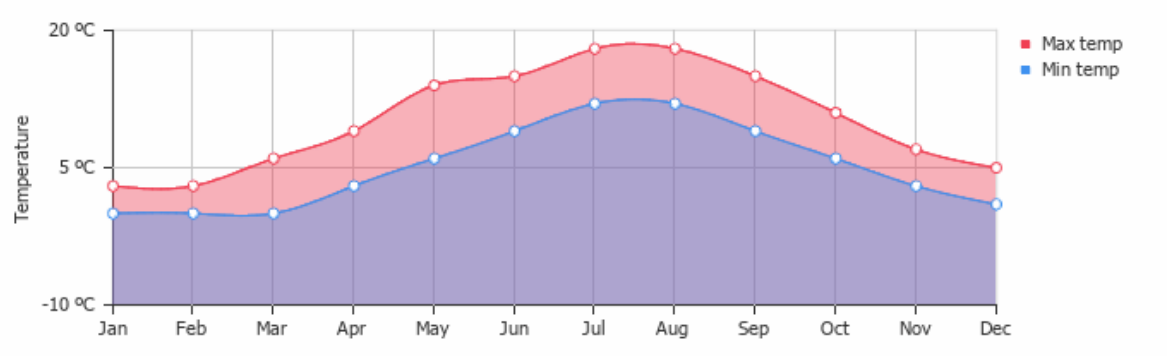

Figure 2.4: Average day and night temperature (Climate, 2019)

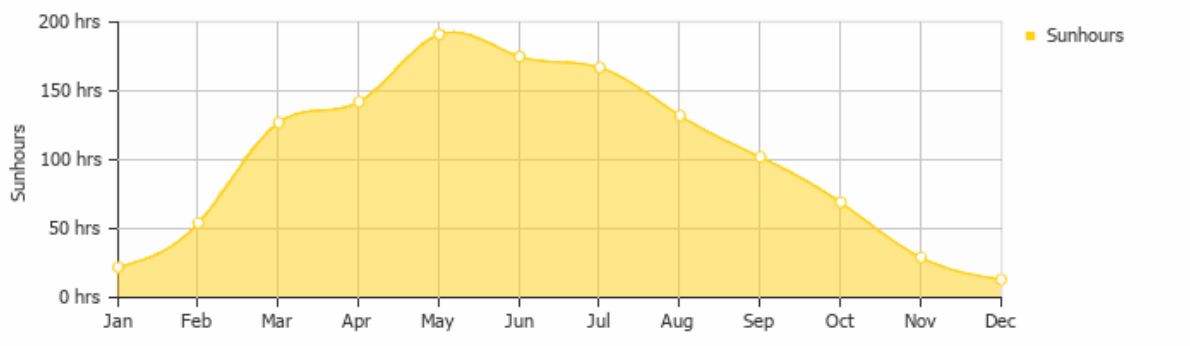

Figure 2.5: Monthly hours of sunlight (Climate, 2019)

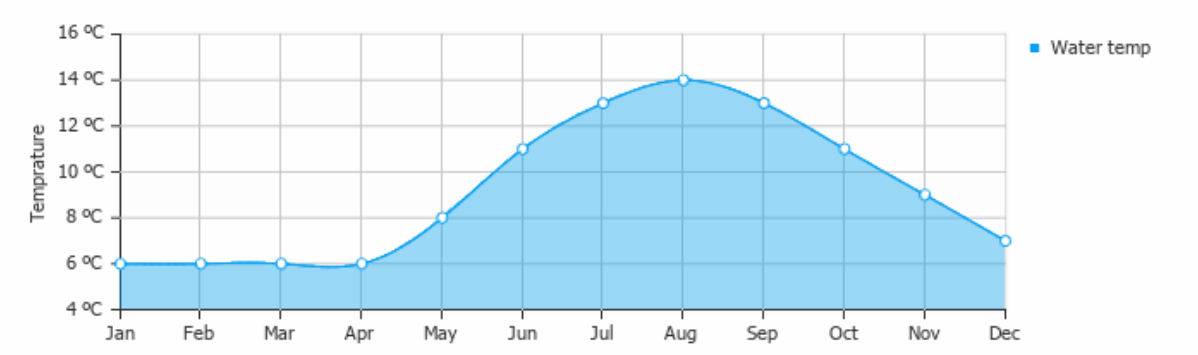

Figure 2.6: Average water temperature (Climate, 2019)

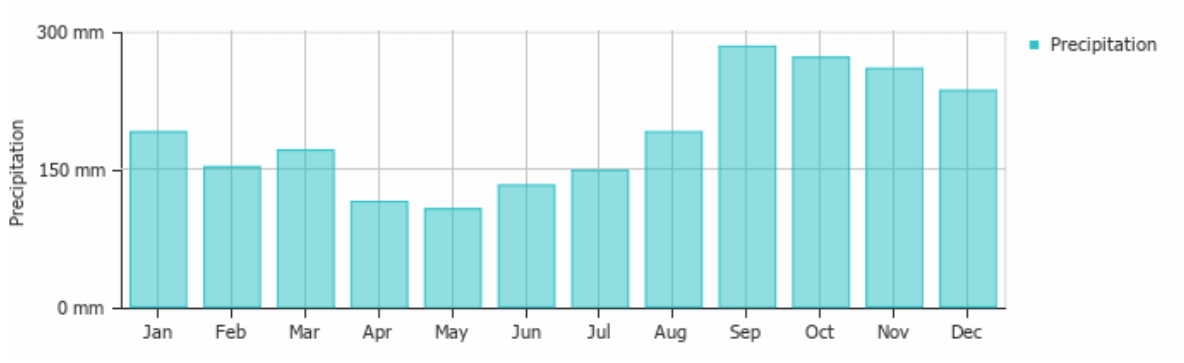

Figure 2.7: Monthly precipitation (Climate, 2019)

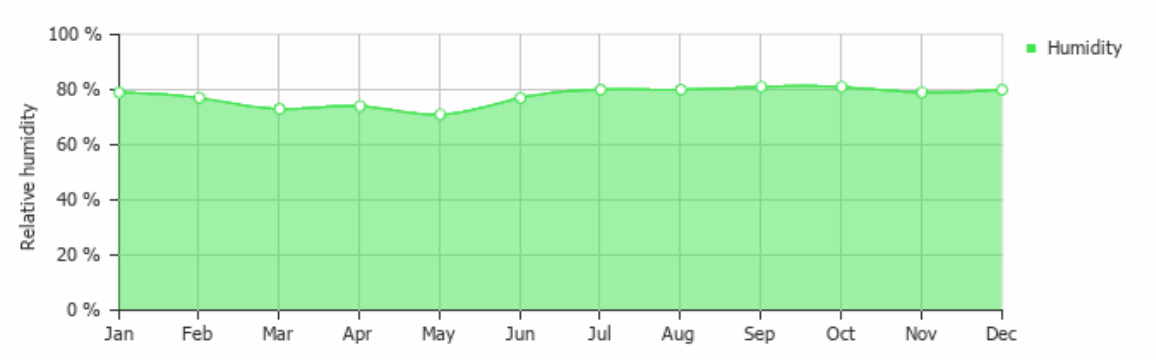

Figure 2.8:Average humidity (Climate, 2019)

In 2019, Hjelmeland recorded a highest temperature of 25.5°C and a lowest of -2°C. The longest day recorded was on June 20th and the shortest day on December 21st. The daylight average is around 10 hours. The water temperature is on an average 8-10 degrees but drops down to 6°C during the winter months. May is the driest month, whilst September is the wettest month, with the average annual precipitation is 1137 mm. The humidity is almost constant every month, with an average annual percentage of 78%

Comparing different aging test protocols and parameters based on literature

Paper	Materials	**Methods**	**Standard**	**Cycle used**	**Testing time**
(Kaynak and Sarı, 2016)	Polylactic acid Tester: QUV	**UV lamp setting:** Fluorescent lamps (UVB-313) with 0.49 W/m^2 irradiance (at 310 nm) **Temperature:** 70°C **Cond temperature:** 50°C	ASTM G154	UV exposure for 8 hours at 70°C followed by 4 hours of dark condensation at 50 °C	50, 100, 150 and 200 h
(Yang et al., 2014)	PVC Tester: QUV	**UV lamp setting:** Fluorescent lamps (UVA-340) with wavelength of 365 nm to the solar cut-off of 295 nm	ASTM G154	UV exposure for 8 hours at 50 ± 3 °C followed by 4 hours of dark condensation at the same temperature	1920h
(Gulmine et al., 2003)	Polyethylene Tester: QUV	**UV lamp setting:** UVB with 0.60 W/m^2 irradiance (at 313 nm) **Temperature:** 60°C	ASTM G154	UV exposure for 8 hours at 60°C followed by spray for 4 hours at 50°C	12, 24, 50, 100, 200, 400 and 800 h
(Gulmine and Akcelrud, 2006)	Cross linked polyethylene Tester: QUV	**UV lamp setting:** UVB with 0.60 W/m^2 irradiance (at 313 nm) **Temperature:** 60°C	ASTM G154	UV exposure for 8 hours at 60°C followed by spray for 4 hours at 50°C	12, 24, 50, 100, 200, 400 and 800 h

(Mathieu and Laurent, 1996)	Plasticized PVC Tester: QUV	**UV lamp setting:** Fluorescent lamps (UVB-313) with 0.49 W/m^2 irradiance (at 310 nm) **Temperature:** 70°C **Cond temperature:** 50°C	ASTM G154	UV exposure for 6 hours at 70°C followed by 6 hours of streaming condensation water at 40°C	200h

2.7 Non-Destructive evaluation technique

2.7.1 Hyperspectral imaging

Hyperspectral imaging is a novel and promising technology that integrates spectroscopy and machine vision to furnish spatial and spectral information simultaneously from the material or object that is being analysed (Calvini et al., 2017). In HSI, the unique colour signature of the object under observation can be identified. Unlike other optical technologies that scan for single colours, HSI distinguishes the full colour spectrum in each pixel. Hence, it can provide spectral information in addition to 2D spatial images(Schneider and Feussner, 2017). Hyperspectral imaging combines two mature technologies, spectroscopy, and imaging. Unlike ultraviolet and multispectral cameras, the hyperspectral camera records images using the whole electromagnetic spectrum, which is used to identify objects and surfaces(Chang, 2003). While the human eye is limited in capturing wavelengths in 3 bands (red, green, blue) within the visible spectrum of 400-700nm. Hyperspectral cameras can capture wavelengths anywhere between 350-

1700nm with ease and the spectral images that are captured by HS imaging can record hundreds of continuous spectral channels compared to the spaced 5-10 bands that are captured by multispectral cameras. This feature allows for superior analysis and the visualisation of material surface, texture, and structure. Hyperspectral Imaging (HSI) is a hybrid technique that combines reflectance spectroscopy with digital imaging. It was first introduced in astronomy and has a wide range of applications such as, remote sensing, paints and coatings, cultural heritage, and medical sciences. This combination of spectroscopy and imaging results in a three-dimensional (3D) space, called a spectral cube, which consists of one spectral and two image dimensions. The benefits from the spectroscopy point of view, is that the 3D cube consists of millions of different measurement points. From the imaging point of view, three colour vision (trichromatic imaging) is extended to hundreds of colour components. Moreover, such a combination enables mapping of areas with similar spectral characteristics.

2.7.1.1 Basic operation principle

To study the reflecting or transmitting light through the target, a spectrometer is required. A spectrometer is a device that splits incoming light into a spectrum. Hyperspectral imaging uses this concept to measure these spectra

The principle behind HSI is that each of the object's molecules are uniquely sensitive to light at different wavelengths(Sendin et al., 2018). HSI produces pixel-by-pixel spectrum of each individual pixel within the image and can be described as a two-dimensional spatial image (x and y) at each one-dimensional wavelength (λ), as well as recording the one-dimensional spectrum (λ) at every two-dimensional pixel (x and y)(He et al., 2013)

The setup includes a lens and an aspheric mirror that focusses the incoming light from the area imaged. The light is then focussed onto a slit that specifies the field of view. Behind this slit is another aspherical mirror that collimates the incident light into a grating to be dispersed. The grating is followed by an objective lens that would focus the light onto a charge coupling device, which also acts as a detecting array to measure the amount of incident light.

2.7.1.2 Acquisition methods

Whiskbroom:

Commonly referred to as point-scan imaging, where the pixels in an object are scanned one at a time. The light from the pixel is scattered by a scattering element such as a diffraction grating or prism. Then there is a detection element for the scattered wavelengths to be recorded. This method renders a very stable resolution spectrum but is time consuming(ElMasry and Sun, 2010).

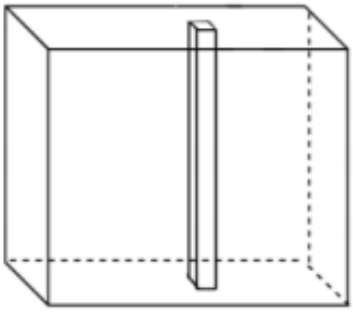

Figure 2.9: Whiskbroom scanning

Pushbroom:

Pushbroom, referred to as the line-scan imaging is the most common method that is used to conduct spectral imaging. In this, a row of pixels is imaged simultaneously and linear scanning provides spatial dimension(Skauli et al., 2011). In relation to the whiskbroom, the Pushbroom uses the same scattering element and principle. However, this method uses a two-dimensional scattering element and a two-dimensional detection array. The Pushbroom is faster than the whiskbroom.

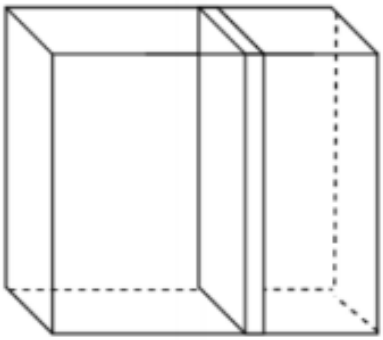

Figure 2.10: Pushbroom scanning

2.7.1.3 Image processing:

After acquiring the data, imaging processing must be done to extract the useful information. Generally, a hyperspectral image contains hundreds of spectral pixels, with each pixel storing information of recorded spectral bands. The recorded information is very large, multidimensional, and often occupy a lot of storage space in terms of data. Visual interpretation is difficult without any form of processing. Enhancing features like edges and sharpening, along with removing noise are some of the processing steps that make the interpretation easier.

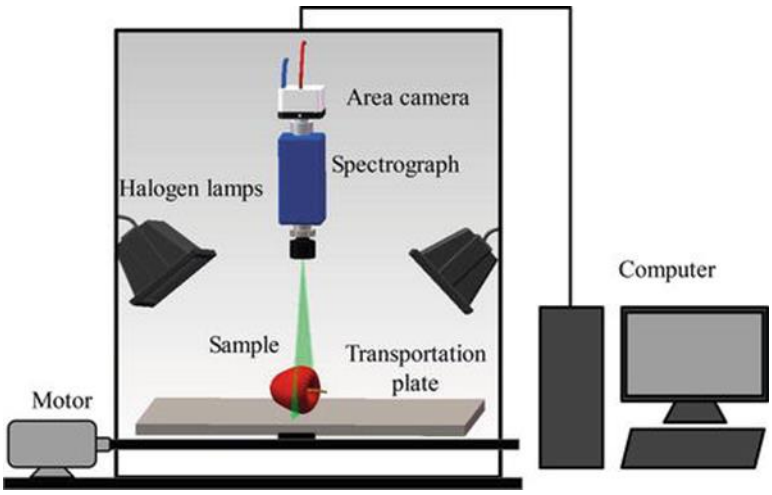

Figure 2.11: Hyperspectral camera setup

3.Methods and Materials

This chapter introduces the various methods and materials that are utilised in this study, these include the materials being tested, mechanical testing methods, characterisation techniques, metrological methods.

3.1 The Process

Step 1: Ageing

The samples were aged according to L. Banks criteria with a few modifications, allowing for sub-intervals between main intervals to be recorded. The samples were aged in a UV tester by QLAB to simulate and accelerate the natural weathering process. The accelerated aging protocol to determine the aging behaviour of HDPE and the timeline for the testing was based on l. Bank theory(Bank et al., 2003). The test matrix was developed at ASEM Lab with aging spanning over a period of 112 days. Control specimens were tested to benchmark unaged properties later to be compared with aged specimen. The test matrix hence presented in Table:

Table 3.1: Test matrix

Intervals	**Aging time**		**No of Samples at each interval**	**Number of samples used for each test**		
	Days	***Hours***		***Tensile***	***Flexural***	***Hyperspectral imaging***
1	28	672	15	5	5	5
2	56	1344	15	5	5	5
3	84	2016	15	5	5	5
4	112	2688	15	5	5	5

Step 2: Storage and sample preparation

The aged samples were taken out at each aging interval and stored in the fridge to retard the aging process. Once the samples from each aging interval were taken out and stored, they were labelled according to their age and collectively placed in Ziploc bag overnight to bring them up to room temperature and prevent the absorption of atmospheric moisture.

Step 3: Preliminary tests/analysis

Dimensions measurements:

The samples at each age interval were measured using a vernier calliper to determine the thickness and width and its variance across different age intervals.

Weight measurements:

The samples at each age interval were measured using a precision scale to determine moisture absorption at each stage (if any) and the variance across the intervals

Step 4: Testing

Destructive testing:

Tensile testing:

The tensile tests were carried out in accordance with ASTM D638. The setup includes an electromechanical universal testing machine Instron 5960 at a room temperature of 23 C and a RH of 48%. The parameters that would be determined from testing include Youngs modulus, Tensile strength and toughness. The testing is done at a testing rate of 10mm/min.

Flexural testing:

The flexural tests were carried out in accordance with ASTM. The setup includes an electromechanical universal testing machine with a 3-point bending setup. The parameters that would be determined from testing include Flexural modulus and flexural strength. The results from both the tests would be plotted to determine the material behaviour change across the aging intervals. The testing is done at a rate of 10mm/min

Non-Destructive testing:

Hyperspectral imaging:

The specimens at each aging interval would be scanned using a hyperspectral camera to obtain spectral information about the material surfaces and potentially determine any effects of aging.

Step 5: Results and Discussion

The results are plotted, tabulated and the observed findings are reported, and a suitable case is made for the findings.

3.2 Sample preparation

400 dog-bone samples of HDPE supplied by SINTEF Raufoss Manufacturing were fabricated by means of injection moulding according to the ASTMD638 tensile testing of polymers criterion. 240 samples were taken out from the batch and installed in two testers, 120 samples each, both under similar testing conditions. These samples were used for tensile testing and mounting in the accelerated UV weathering chamber. At each aging interval, 15 samples would be taken out, out of which 5 would undergo hyperspectral imaging followed by tensile testing, 5 would undergo flexural testing. Following the testing, the properties would be analysed, along with the degree of degradation at each interval.

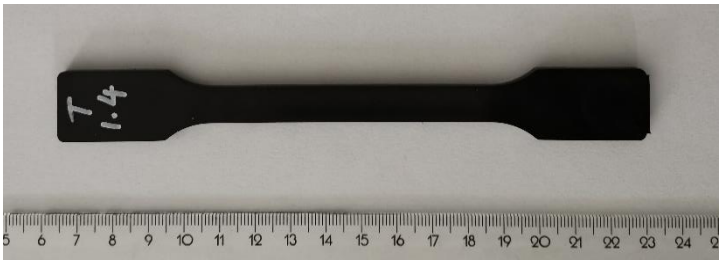

Figure 3.2: A dog bone tensile specimen used in this study

3.3 Accelerated aging chamber/tester:

The artificial accelerated aging process is done by means of a Universal weathering chamber. The tester reproduces the damage caused by external weathering agents such as sunlight, rain and dew(Ketola et al., 1994). The QUV accelerated weathering tester replicates the damage that is caused by sunlight, dew, and rain. The tester can reproduce the damage that occurs over months or years in an external environment(QLab, 2017). To stimulate the weathering that occurs outdoors, the chamber subjects the material to alternating cycles of moisture and UV light at controlled temperatures. It simulates the effect of natural sunlight and artificial irradiance using fluorescent UV lamps in the UVA, UVB, and UVC regions of the spectrum and simulates dew and rain with condensation and/or water spray. The tester allows for using multiple combinations of UV and moisture based on the end user requirements(QLab, 2017).

Figure 3.2: QUV Accelerated weathering tester (QLab, 2017).

The test was based on the ASTM G154 standard of using UV lamps to age non-metallic materials. The testing parameters and order of events were modified according to the pre-determined climatic conditions to simulate the year-round conditions in the Norwegian coastline. The test was conducted for a period of 112 days and the specimens were taken out at intervals of 28, 56, 84, 112 days to undergo uniaxial tensile testing, flexural testing, and hyperspectral imaging. The aging protocol followed is an excerpt from the proposed model of (Bank et al., 2003) to predict the lifetime of mechanical properties of polymers in the long-term. Once the sample holders were installed, they were swapped into different positions once every two weeks to ensure uniform exposure to the elements. Irradiance calibration was done every 500 hours using a UC10/UV sensor to ensure accuracy and uniformity in irradiance. The samples at each 28-day intervals were taken out, bagged in airtight Ziploc bags, and stored in the fridge to retard the aging process. The lamps used for the testing were UVA at an irradiance of .89 W/m^2 at a wavelength of 340nm as they are the best available simulation for the crucial short-wave UV region(QLab, 2017).

3.3.1 Designing a suitable accelerated weathering cycle:

The reason behind choosing a location, is to identify the fish farms using Plasto's product in their fish farms and to design a test cycle based on real-life weather conditions experienced in Hjelmeland, Norway. AKVA Group utilises polymer products manufactured by Plasto, which includes cages, pens, brackets, and walkways etc.

The collaboration between Plasto and AKVA Group was established in 2008 to develop a long-term mutual relationship. The agreement entailed sharing technological developments, collaboration in mould design and manufacture, product and production process(Charter, 2018). Majority of the work done revolves around new products and technology that can be utilised in fish farms and as of June 2017, AKVA Group has committed to contribute to Plasto's ongoing work of analysing risks and opportunities of using recycled polymer products in fish farms.

The geographical location selected for this case study is Hjelmeland, which is home to Sterling White Halibut AS. This fish farm is in Southwestern Norway, rooted in the cold pristine waters of the Ryfylke fjords. This serves as the optimal place for farming fish and the climatic conditions chosen for this study has been based on the prevailing climate in Hjelmeland.

Hjelmeland has 2 types of climates prevailing, the oceanic climate and continental climate. The average annual temperature for Hjelmeland is 3 degrees and it receives about 1137 mm of rain in a year. It is dry for 100 days a year with an average humidity of 78% and an UV-index of 2(Climate, 2019).

The conditions set in the chamber were as follows:

- UV at .89 W/m2 for 6 hours at 80°C
- Condensation for 4 hours at 50°C
- Spray for 2 hours at room temperature

3.4 Uniaxial Tensile testing:

Uniaxial tensile tests are the most optimal method for the investigation of ultimate strength and other stable mechanical properties, commonly referred to as engineering stress-strain curves. The mechanical properties that are derivable from the uniaxial tensile test include: Strength, in the form of yield stress and ultimate tensile strength, The stiffness of the material (young's modulus), The toughness of the materials i.e. energy absorbed per unit volume up to fracture and ductility of the material, i.e. elongation up to fracture. 3.5.2

3.4.1 The standard

The standard test ASTM D638 is performed by applying a tensile force to a sample specimen and measuring multiple properties of the specimen under stress. It is conducted using a universal testing machine which is electro mechanical in nature (also called a tensile testing machine) at tensile rates ranging from 1 to 500 mm/min until the specimen fails (yields or breaks). The properties of the curve that are of interest for the study are as follows:

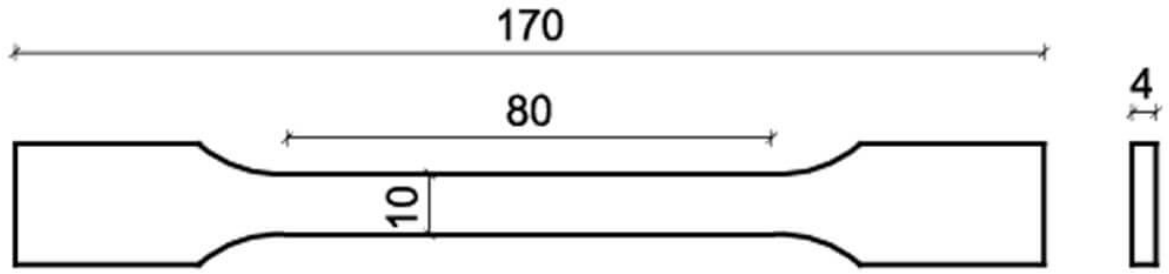

Figure 3.3: Tensile test standard dog bone specimen (Instron, 2016)

Properties measured:

- Tensile strength: the amount of force that can be applied to a plastic before it yields (stretches irreparably) or breaks.
- Elastic modulus: how much a material can deform/stretch in response to stress before it yields. Modulus is a measurement of the material's stiffness(Callister, 2007).
- Toughness: The amount of energy absorbed by the material before it fails, area under the curve in effect.
- Lower tensile strength: The lower value of stress, after the ultimate tensile stress, but before the material starts to fail.
- Stress at break: The stress experienced when the material fails.

3.4.2 Effect of strain rate

A loading rate of 10mm/min was chosen as it allows for the normal mechanical behaviour, preventing premature failure and errors in the results. The work done by (Abdelkader et al., 2015)corroborates this choice of loading rate after experimenting with 3 different rates of 5, 10 and 50 mm/min and how it affected the mechanical behaviour of HDPE. 5 and 10mm/min had similar graphs, whereas 50mm/min had a catastrophic brittle failure coupled with a high ultimate stress. Since the behaviour of the 5 and 10mm/min were similar, the 10mm/min was chosen as it consumed lesser time for each test.

3.4.3 Setup and testing:

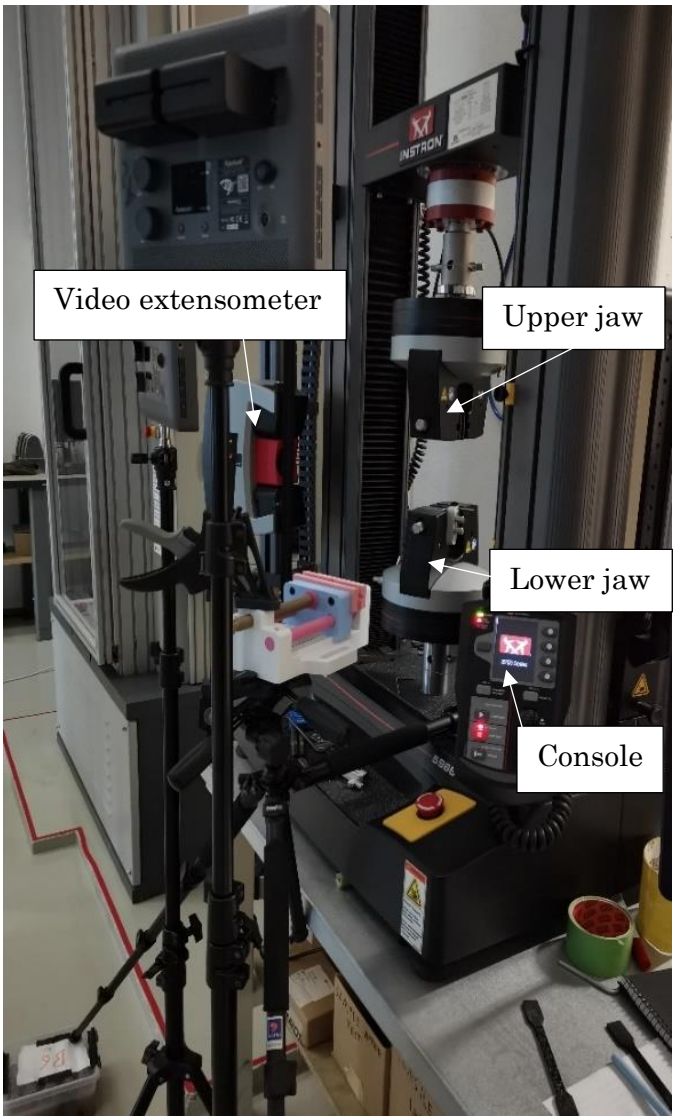

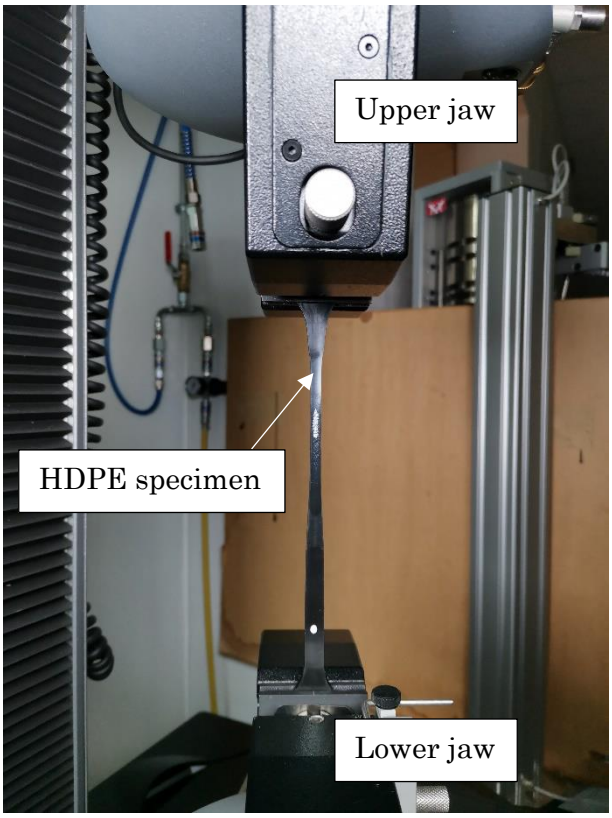

Figure 3.4: Setup for the tensile test

The tensile tests were carried out on a Universal testing machine Instron 5960. The width and the thickness of the specimens were measured using a sliding calliper prior to testing. The ASTM standard specimens were fixed at a constant distance between the grippers and preloaded with 5N to remove any slacks and to initiate a state of tension. The test was performed according to ASTM D 638 and initiated at an elongation rate of 10mm/min and the elongation was recorded on both the mechanical and video extensometer after specimen failure. The average values of 5 specimens were reported.

3.4.4 Data Analysis:

During the tensile test, the force and the crosshead displacement were measured by an internal transducer and obtained as raw data from the Instron testing machine. From the force and displacement values,

The tensile stress was measured using the formula:

$$stress = \frac{F}{A}$$

Where:

F - Force

A – Area of cross section (width * thickness)

The tensile strain was measured by using the formula:

$$strain = \frac{\Delta L}{L}$$

Where:

ΔL – Change in length

L – Original length

The Ultimate tensile strength was measured by isolating the highest value on the tensile stress-strain curve and the elastic modulus was calculated by constructing a line intercepting the curved region before it reaches the peak, where the line has a regression value of almost 1. The slope of this line was obtained from the equation of the line and reported. The lower tensile stress was measured by isolating the lowest value of stress after the necking and before the strain hardening region. The stress at break was measured by isolating the value of stress just before the material fails.

The modulus of toughness is calculated as the area under the stress-strain curve up to the point of failure. A precise calculation of the total area under the stress-strain curve to determine toughness is a bit difficult. However, a rough approximation can be made by dividing the stress-strain curve into a rectangular and triangular sections, as seen in the figure below.

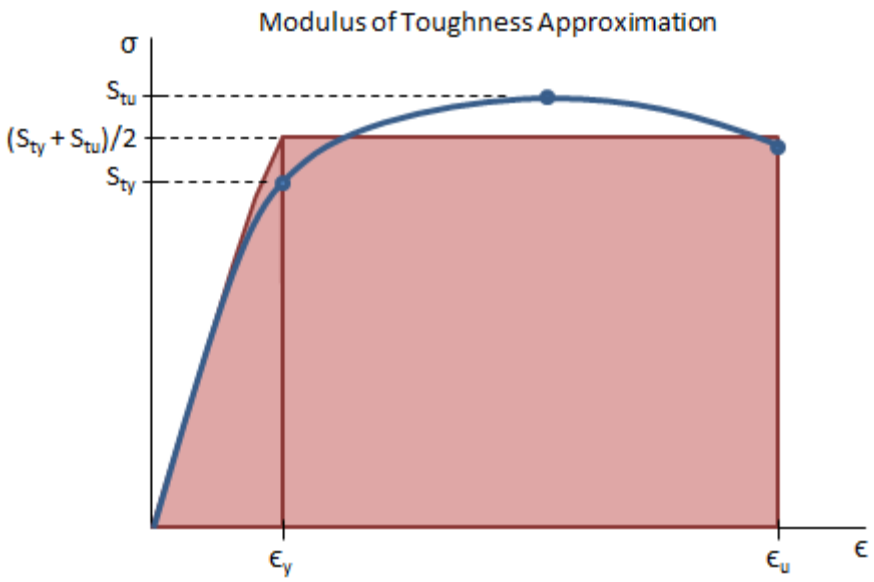

Figure 3.5: Calculation of the modulus of toughness(Mechanicalc, 2013).

The modulus of toughness can be approximated as:

$$u_t = \left(\frac{Sty+Stu}{2}\right) \cdot \left(\varepsilon_u - \frac{1}{2}\varepsilon_y\right)$$

$$= \left(\frac{Sty+Stu}{2}\right) \cdot \varepsilon_u \left(\frac{Sty+Stu}{2}\right)^2 \cdot \frac{1}{2E}$$

where S_{ty} is the tensile yield strength, S_{tu} is the tensile ultimate strength, ε_y is the strain at yield, ε_u is the ultimate strain (total strain at failure), and E is the elastic modulus. Hence the toughness is obtained by means of the above calculation(Mechanicalc, 2013).

3.5 Flexural testing

Flexural testing is used to measure the force required to bend a beam of plastic material and determines the resistance to flexing (stiffness) of a material. Flexural modulus is an indication of how much the material can flex before permanent deformation(Shrivastava, 2018). The common utility of a flexure test is to measure flexural strength and flexural modulus. Flexural strength is the maximum stress the outermost fiber experiences on either the compression or tension side of the specimen. Flexural modulus is calculated from the slope of the stress vs. strain deflection curve. These two calculated values can be used to estimate the stiffness of the material and its resistance to bending forces.

The Instron machine used to carry out the tensile test is utilised to perform the 3-point flexural test to calculate the flexural strength of the specimens and the test is carried out a at room temperature. The samples for flexural testing were fabricated by machining the dog bone samples into suitable specimens according to the ASTM-D790-17(Dhinesh et al., 2020). The specimens for the flexural test were developed from the dog-bone samples by milling them to the suitable standard size. The flexural properties of the machined standard sample were compared against the unaltered dog-bone sample and a dog bone sample with the edges trimmed off. The hypothesis is that, if all three iterations of the specimen record similar flexural properties, then machining can be omitted, as it is an unnecessary step that is time consuming. After conducting tests on the three samples it was evident that the results were identical. Since the results were identical, the dog bone sample was used in all the cases. At each aging/testing interval 5 dog bones were taken out, machined, and tested on a 3-point bending setup and the values were recorded. The average of the 5 results were taken and reported.

3.5.1 The standard:

ASTM D790 is a standard that measures the flexural properties of a material under bending strain or deflection. The test is performed on a universal testing machine, using a three-point setup at a rate which is proportional to the depth of the specimen. The parameters that are determined, include:

- Flexural modulus – It is the slope of the initial linear portion of the load deflection curve and is a measure of the material's stiffness
- Flexural strength – The measure of maximum flexural stress obtained during bending.

The standard ASTM D790 is chosen due to its relevance to the specimen dimensions and material used. For materials that are greater than 1.6mm in thickness (4mm in this case), the specimen width is not to exceed one fourth of the support span for specimens greater than 3.2 mm in depth. The specimen also must have at least 10% of span length as overhang on each side, no lesser than 6.4mm on each end. The aspect ratio that is utilised for this standard is 16:1. The specimen that is used for testing in this case is 10mm in width and 4mm in thickness, and it has more than 10% overhang on both sides, thereby matching all the prerequisites of the ASTM D790 standard.

3.5.2 Setup and testing:

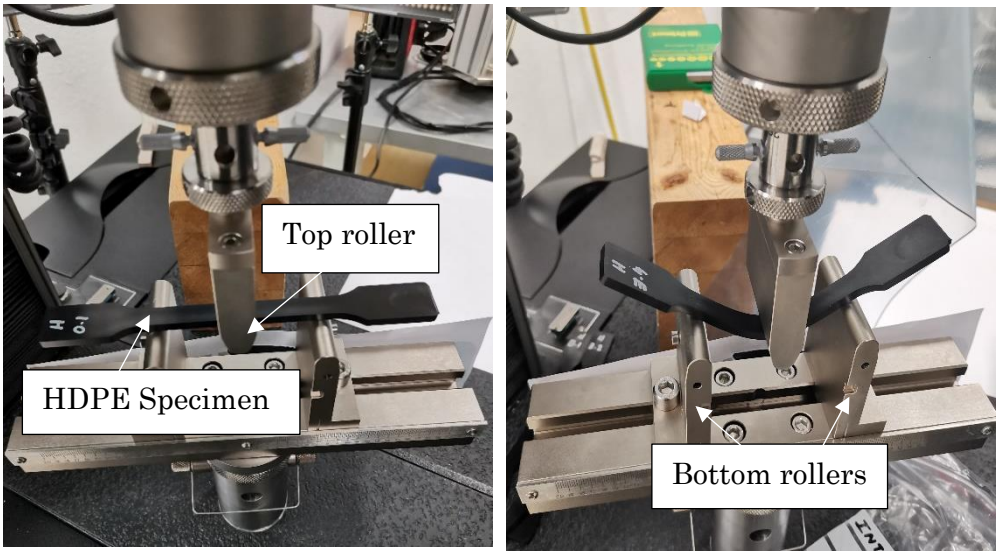

Figure 3.6: Setup for the 3-point bend test

The dimensions of the dog bones were measured, and a marking was made on the centre point of each specimen along with a centre point marking on the wedge to maximise the accuracy and improve the consistency of the results. The specimen was placed in between the rollers and aligned with the centre point before the forces were balanced and a force was applied. The experimental result was recorded as the reaction force versus the middle deflection of the specimen under a monotonic bending load, to obtain the actual flexural stiffness response.

3.5.3 Data Analysis

In the three-point bending test, the force and the crosshead displacement were measured by an internal transducer and obtained as raw data from the Instron testing machine. From the force and displacement values, the stress was measure using the formula:

$$\sigma_{\max} = \frac{3FL}{2bh^2}$$

Where:

F- Force

L – Support span

b – Specimen width

h- Specimen thickness

The flexural strength was measured by isolating the highest value on the flexural stress-strain curve and the flexural modulus was calculated by constructing a line intercepting the curved region before it reaches the peak, where the line has a regression value of almost 1. The slope of this line was obtained from the equation of the line and reported.

3.6 Hyperspectral imaging

In this experiment, the spectral image information of experimental samples is collected by using HSI system consisting of a hyperspectral camera, an illumination system, a computer, and an aluminium frame.

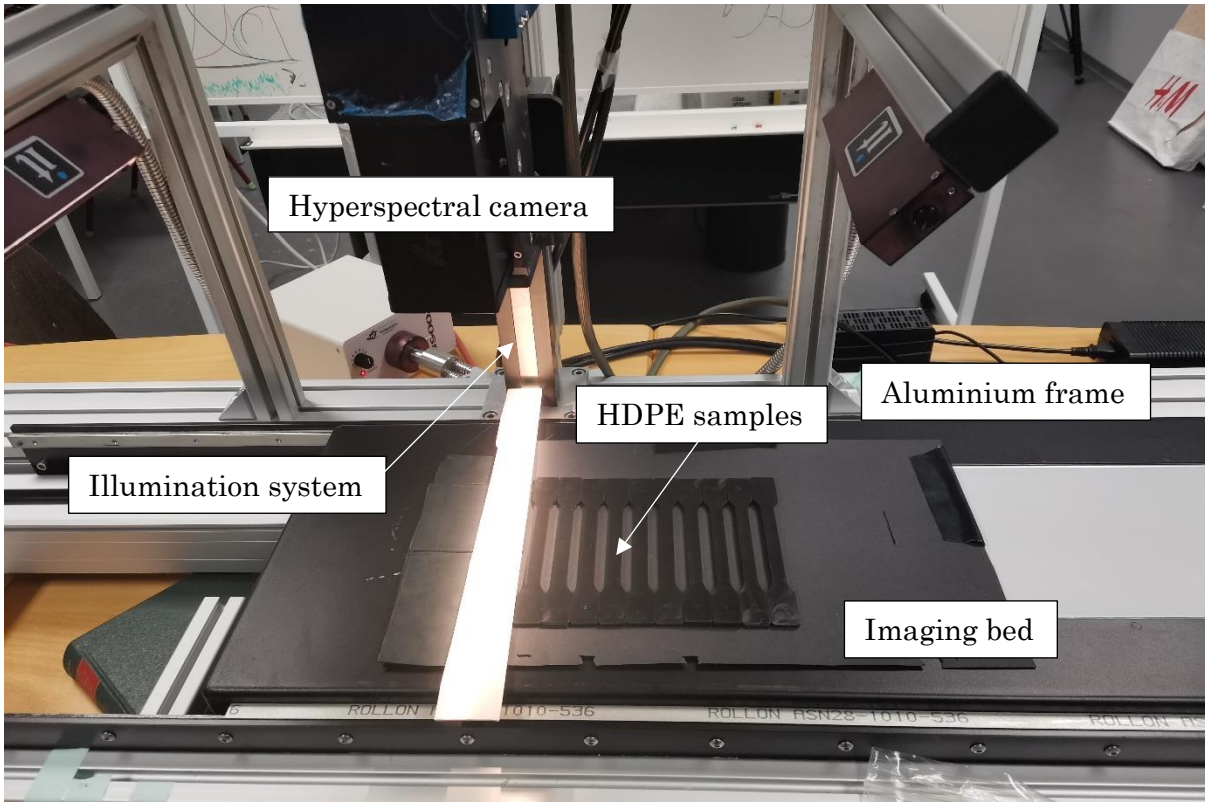

Figure 3.7: Hyperspectral imaging setup

A pushbroom HySpex VNIR-1800 hyperspectral camera produced by Norsk Elektro Optikk has been used to capture all the HS images included in this research work. This line scanner deploys a diffraction grating and results in generating 186 images across the electromagnetic spectrum, from 400nm to 1000nm, at steps of approximately 3.19nm. The focus of the optics is set to 30cm, which translates into a field of view of 10cm and allows to reach an optical resolution of approximately 0.06 mm. The objects are illuminated by a halogen Smart Light 3900e produced by Illumination Technologies, guided on the scene via 2 fiber optics, projecting lights at 45° in respect to the camera. At each acquisition, a Spectralon ® calibration target with a known wavelength-dependent reflectance factor is included in the scene. The target will serve to estimate the illumining spectrum and to compute the reflectance at the pixel level. The HySpex software enables the user to select

an option that performs radiometric correction in real time, correcting the output accounting for the sensor's error response and dark current errors (Skauli, 2012). By performing flat field correction (Kokka et al., 2019), the errors related to spatial non-uniformity are taken care of.

Different materials have different spectral fingerprints and can be identified by their spectral signature. One of the advantages of spectral imaging is the ability to distinguish between materials and their positioning and HSI presents itself as a novel technique to characterize polymers and to rapidly obtain results after the images are taken, if its efficacy is proven.

The objective of using spectral imaging is to observe the spectral characteristics of the degraded plastic and correlate the change in spectral properties to the mechanical properties at an interval of aging. Along with the physical testing of materials, the results of the Hyperspectral imaging of the HDPE at different aging intervals would provide for a reliable non-contact method of testing, where the camera can be taken on site to where the fish farm equipment are located and potentially determine the degree of degradation.

4. Results and discussion

This chapter deals with the numerical results and qualitative findings post-aging that are observed. The results are calculated from the raw data obtained from the testing equipment, plotted, tabulated and the findings are justified by means of supporting literature, discussing the observations, correlation with hypothesis to build a case for the results.

4.1 Weight dissolution due to aging:

Table 4.1: Weight distribution across aging intervals (g):

Sample no.	Unaged	28 days	56 days	84 days	112 days
1	8.540	8.527	8.532	8.535	8.513
2	8.557	8.534	8.541	8.532	8.538
3	8.57	8.530	8.535	8.534	8.531
4	8.557	8.545	8.523	8.529	8.521
5	8.563	8.541	8.532	8.518	8.517
6	8.542	8.523	8.530	8.532	8.512
7	8.555	8.531	8.539	8.533	8.539
8	8.56	8.535	8.536	8.538	8.533
9	8.558	8.539	8.521	8.526	8.521
10	8.561	8.542	8.533	8.519	8.518
11	8.541	8.523	8.531	8.531	8.515
12	8.55	8.531	8.540	8.529	8.538
13	8.575	8.530	8.531	8.533	8.532
14	8.551	8.544	8.524	8.527	8.522
15	8.566	8.544	8.533	8.523	8.51

The weights of all the samples were measured after aging, and it was observed that there was a decline in the net weight at each age interval, with a sharp drop at 28 days, followed by a steady decline up to 112 days. There was an overall decrease of 0.38% in the weight of the samples with age.

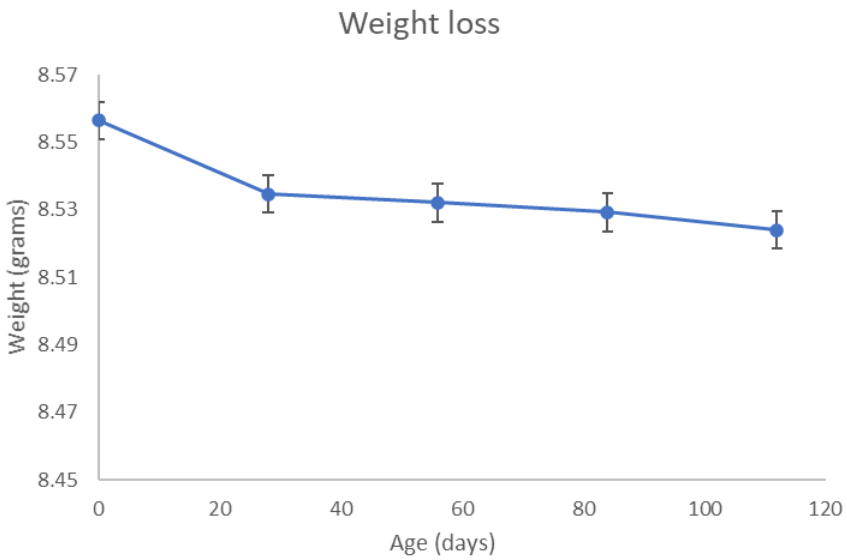

Figure 4.1: Weight loss due to aging

Another study by (Qiao et al., 2009) has explained the weight dissolution by the introduction of oxygen containing carbonyl groups such as C-O, C=O and C(=O)O (Carbonyl and ester groups) due to ultraviolet irradiation. The UV irradiation had also improved the tensile and impact strengths of the irradiated HDPE. The slight weight dissolution has been attributed to slight degradation due to UV, resulting in very little or no aging occurring.

4.2 Tensile property change due to aging

Tensile strength is an important property for analysis of product in terms of its mechanical strength. Uniaxial tensile tests were conducted to investigate the effect of UV on the stress–strain behaviour of HDPE.

4.2.1 Failure of samples at each age interval:

28 days:

Figure 4.2: Tensile failure at 28 days

56 days:

Figure 4.3: Tensile failure at 56 days

84 days:

Figure 4.4: Tensile failure at 84 days

112 days:

Figure 4.5: Tensile failure at 112 days

It is observed that the necking occurs near the top or the bottom, and not near the centre of the specimen, and this is observed across all the aging intervals.

4.2.2 Stress strain curves at each interval:

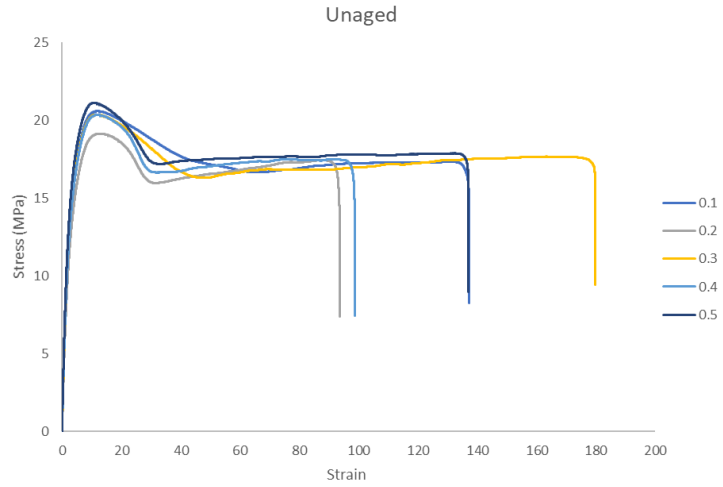

The sample number 0.1 to 0.5 refer to the 5 unaged samples

Figure 4.6: Stress strain curve for unaged samples

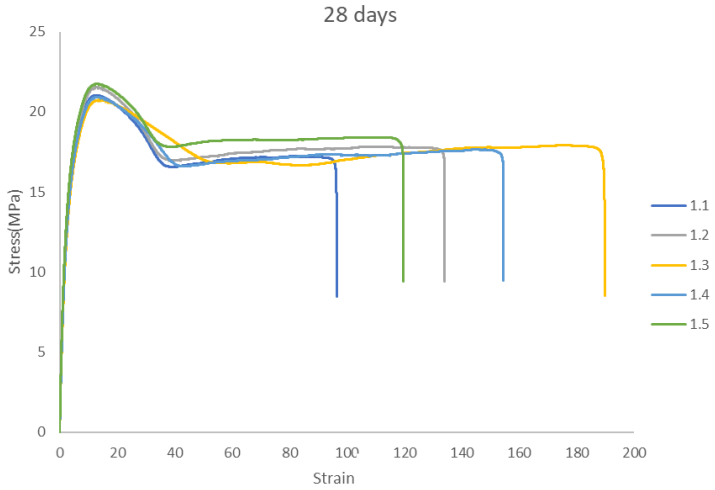

The sample numbers 1.1 to 1.5 refer to the 5 samples taken out at 28 days

Figure 4.7: Stress strain curve for samples at 28 days

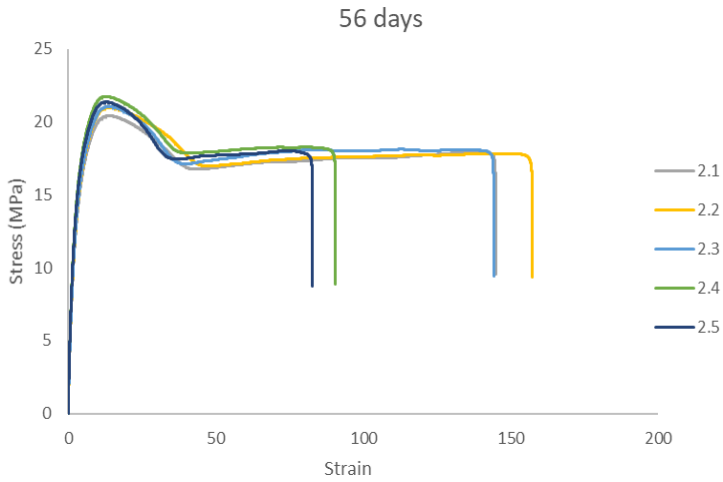

The sample numbers 2.1 to 2.5 refer to the 5 samples taken out at 28 days

Figure 4.8: Stress strain curve for samples at 56 days

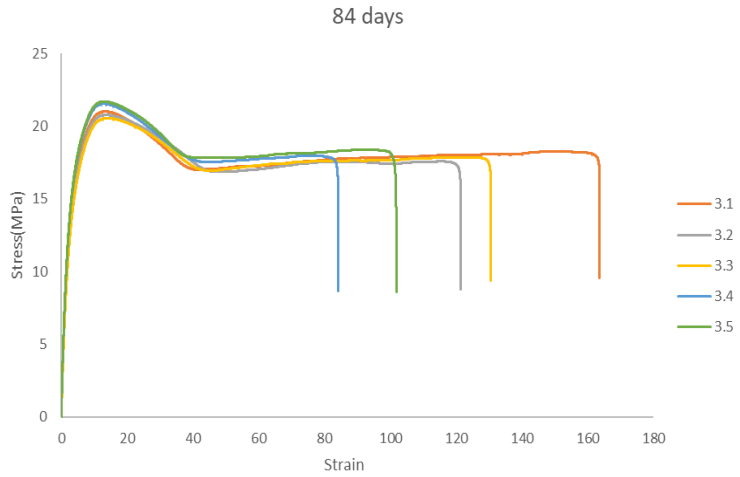

The sample numbers 3.1 to 3.5 refer to the 5 samples taken out at 28 days

Figure 4.9: Stress strain curve for samples at 84 days

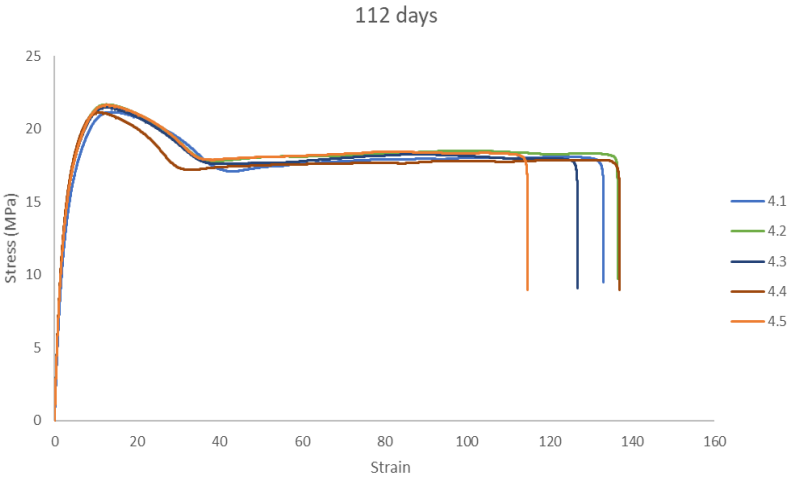

The sample numbers 4.1 to 4.5 refer to the 5 samples taken out at 28 days

Figure 4.10: Stress strain curve for samples at 112 days

4.2.3 Elastic modulus:

The elastic modulus of the samples across the ages were found to gradually increase across the ages up to 4 days, followed by a sharp increase up to 112 days with an overall increase of 10.36%. This phenomenon is due to the increase in crystallinity, micro crystallinity and the subsequent embrittlement of the polymer due to irradiation(Hsueh et al., 2020). It is to be noted that the change in the young's modulus is far lesser and more gradual when compared to the results from the other similar studies. This may be a result of a combination of UV exposure, presence of moisture and an aqueous medium. Since the gage length was primarily exposed to UV, this is the primary area of concern. The study by (Hsueh et al., 2020) also expands upon the surface effect of UV as opposed to the penetration to deeper layers. The photo oxidation that was induced by the UV irradiation increased the modulus of the surface region, possibly via chemicrystallization. These results are due to increase of the incident energy due to the prolonged UV exposure. The UV has sufficient energy to promote C-C chain scissions. The breaking of bonds between carbon atoms and the backbone promotes the formation of double bonds between the neighbouring carbon atoms and even formation of hydrogen bonds between the adjacent chains. All these events cause an increase in Young's modulus and is linked to the increase in crystallinity and stiffness of superficial layers and /or occurrence of crosslinking reactions(Becerra and d'Almeida, 2017).

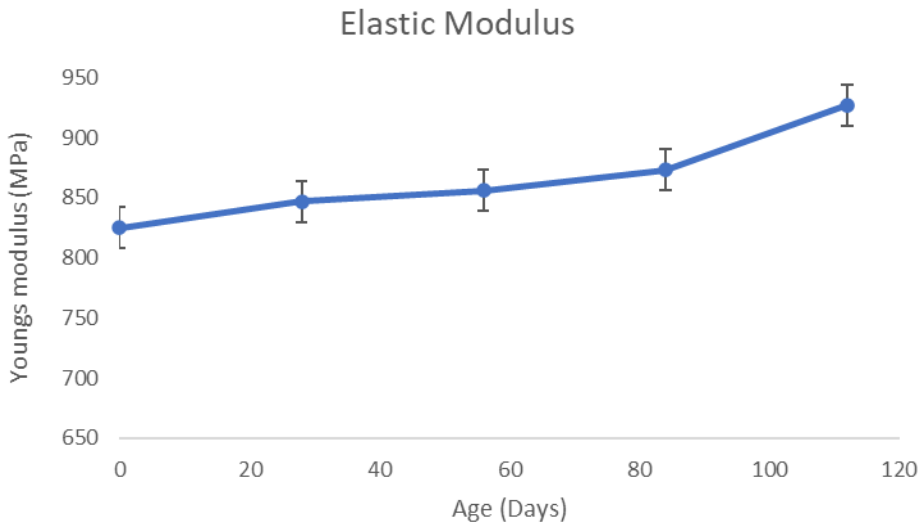

Figure 4.11: Elastic modulus versus age

4.2.4 Ultimate tensile strength

The UTS was determined by selecting the max stress value on the stress strain curve. The Ultimate Tensile strength gradually increases with age with a net increase of 5.45% in 112 days. The tensile strength is seen to climb until 54 days, followed by a drop at 84 days and an increase at 112 days. Tensile strength is a function of crystallinity, and is observed to increase, just as the young's modulus, which is also a function of crystallinity(Craig et al., 2005). This increase in UTS can be explained by the effect of UV light on the bonding that exists in the HDPE. This behaviour is documented by (Bhuyar et al., 2019) who conducted an FTIR analysis on the aged HDPE samples and found out that the chemical structure was altered due to aging and this was confirmed by the transmittance values obtained from the FTIR analysis. The FTIR spectrum contained a high population of bonds whose vibrational energies had correlated incident light. The molar mass of HDPE is known to decrease by means of chain scission accompanied by cross linking during the UV exposure. This is an observed effect along with the reorganization of HDPE molecules into a crystalline phase, resulting in increased crystallinity(Craig et al., 2005).In effect, there is no significant change in the tensile strength of the samples across the ages. A similar study on HDPE geomembranes by (Kiersnowska et al., 2020) involves the accelerated aging of HDPE over 12 months and investigating the effect of aging on the polymer and the tensile strength of the samples was found to increase very slightly when they were aged at a temperature of 75 C, while in this case the HDPE was subjected to accelerated aged with the UV stage at 80 C with a combination of a UV and moisture based cycle.

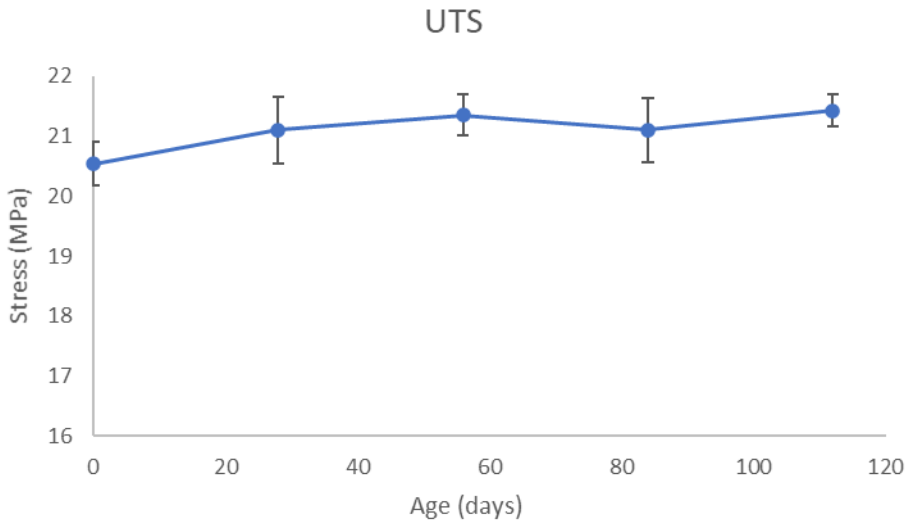

Figure 4.12: Ultimate tensile strength versus age

4.2.5 Lower tensile stress

The lower tensile strength follows a similar trend to the UTS expect for the 84-day mark, where the UTS decreases by 1.1% before a slight increase at 112 days. Overall, the Lower tensile stress increases by 5.78 %, increasing from 16.54MPa to 17.50MPa.

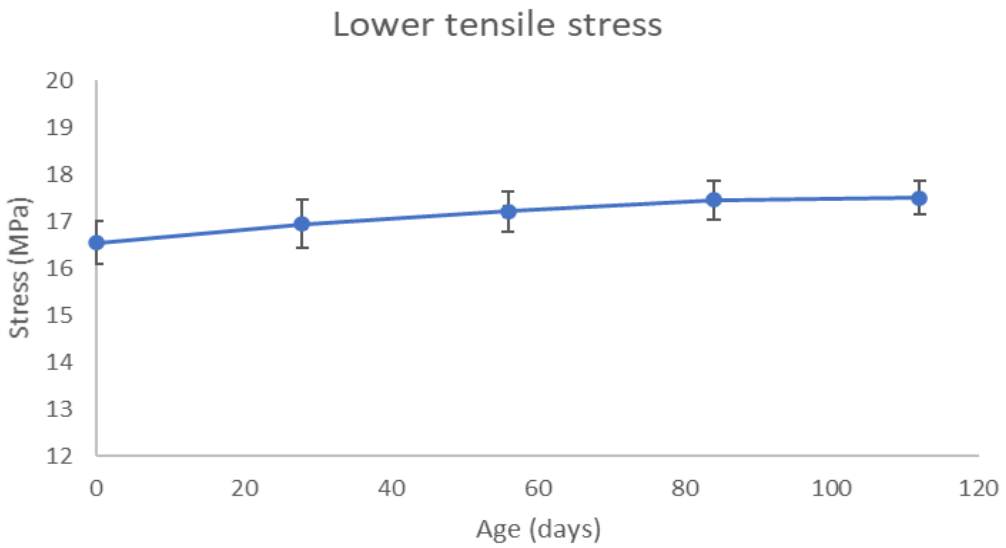

Figure 4.13: Lower tensile stress versus age

4.2.6 Toughness:

There was a drop of 11.63% in the toughness in 112 days. The failure in these varied points can be attributed to defects in the specimen or due to material shape (increased stresses at the edges) or defects due to manufacture (voids/ moulding strain) and also due to the effect of UV radiation. The study by (Hsueh et al., 2020) corroborates this with the decrease of elongation at failure as the exposure time and intensity of the UV radiation was increased. In this case, the intensity of the UV radiation remained constant, but the exposure time was varied at each age interval. The samples were irradiated with alternating cycles of UV and there was an observed decrease in elongation and toughness in the strain hardening region. This is also caused due to the increase in crystallinity, and the subsequent embrittlement of the polymer due to irradiation(Hsueh et al., 2020)

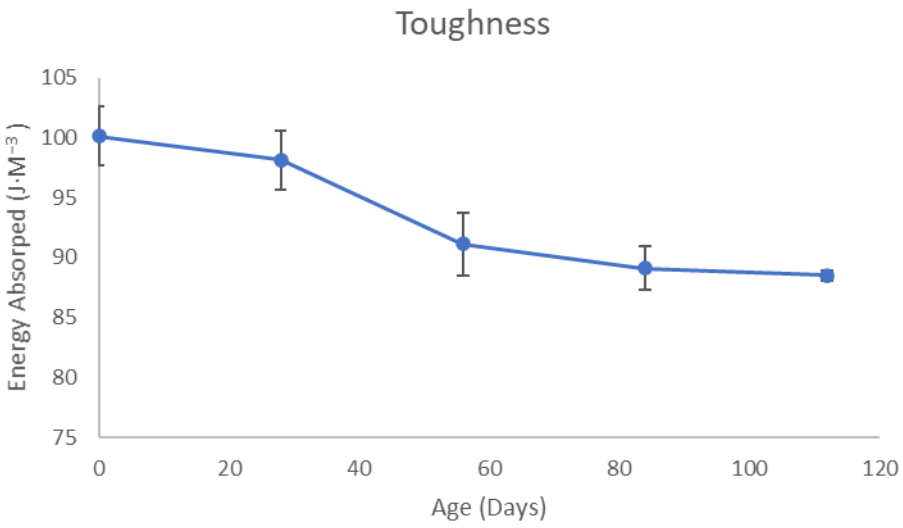

Figure 4.14: Toughness/ Energy absorbed at each age interval

4.2.7 Stress at break:

The stress experienced at break experiences a miniscule decrease of 1.65% in 112 days. After 112 days, the stress at break decrease from 17.75 to 17.48 MPa, with a net decrease of 1.65%. It is also evident that the toughness of the material decreases with each age interval.

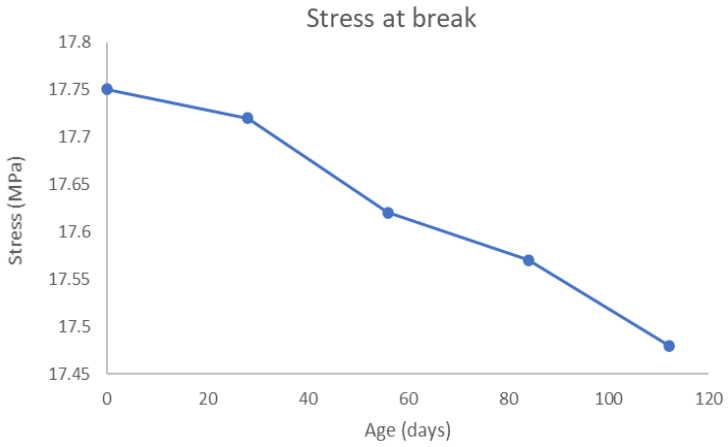

Figure 4.15: Stress at break vs age

4.2.8 Overall tensile property change:

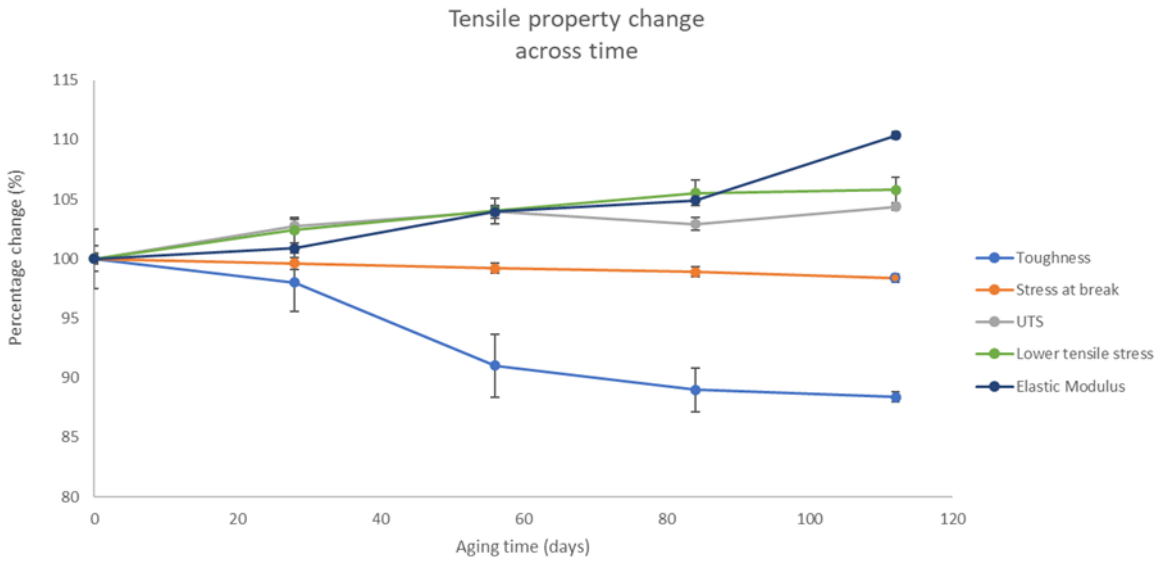

4.3 Flexural Testing

The samples were kept in a refrigerated environment, post aging to retard the subsequent degradation. All the samples were tested at room temperature to ensure the uniformity and consistency of results. The samples that were to be tested by the 3-point bend test and the results were reported and the flexural modulus and flexural strength were calculated and reported.

4.3.1 Stress strain curves

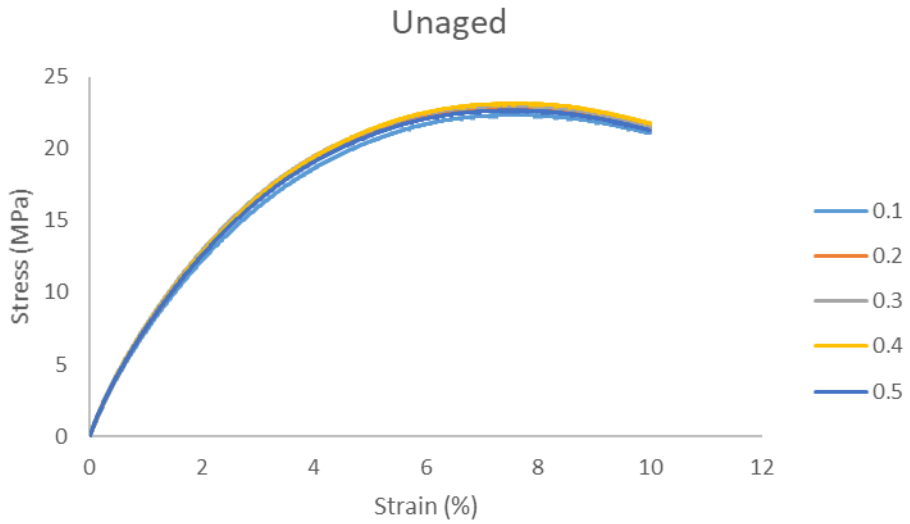

The sample number 0.1 to 0.5 refer to the 5 unaged samples

Figure 4.16: Stress strain curve of Unaged samples

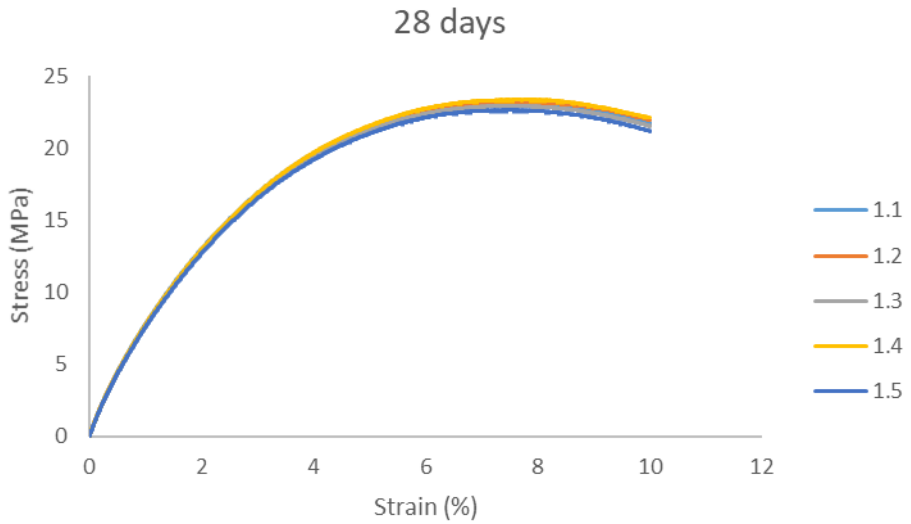

The sample number 1.1 to 1.5 refer to the samples taken out at 28 days

Figure 4.17: Stress strain curve of 28-day old samples

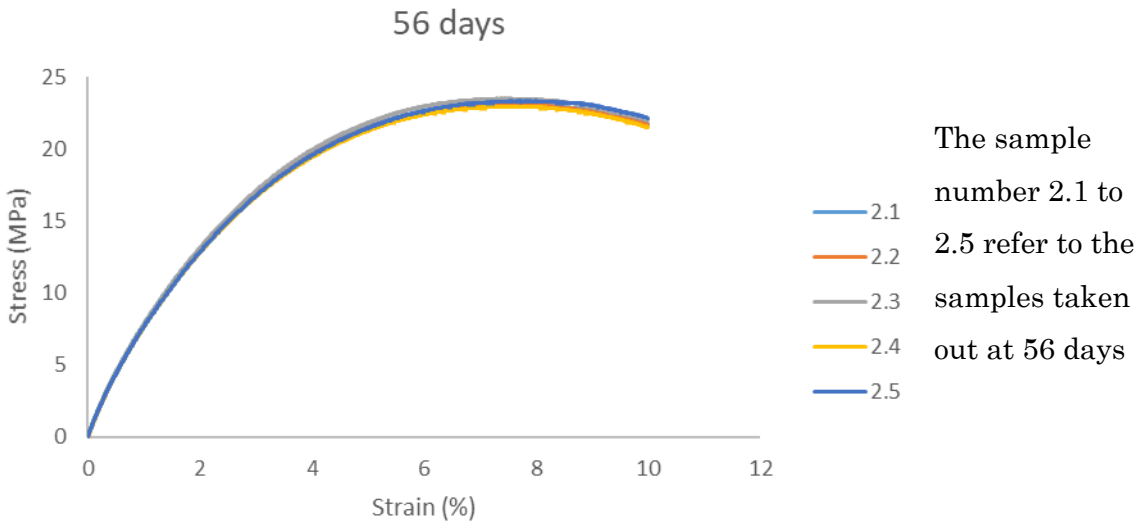

The sample number 2.1 to 2.5 refer to the samples taken out at 56 days

Figure 4.18: Stress strain curve of 56-day old samples

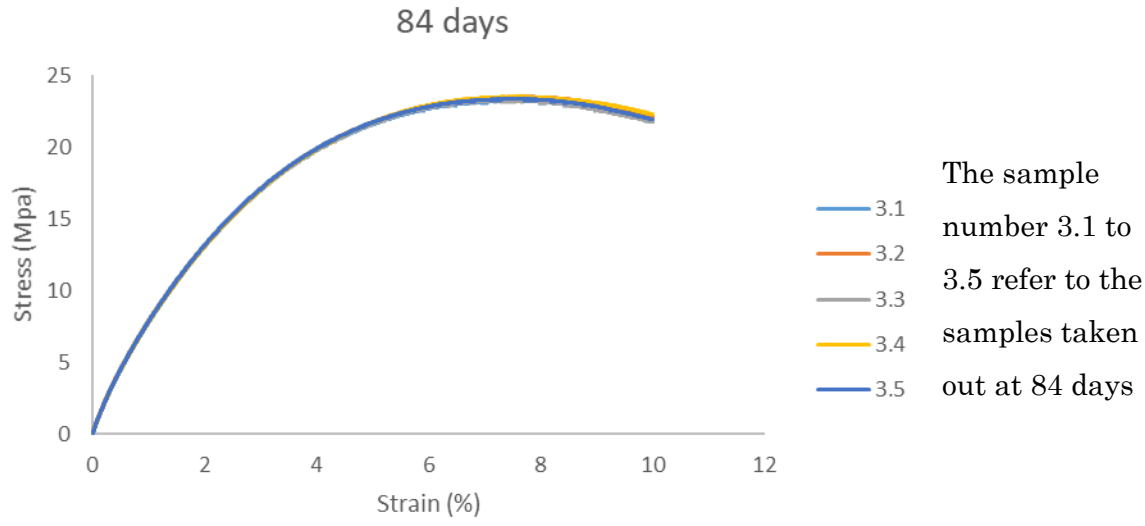

The sample number 3.1 to 3.5 refer to the samples taken out at 84 days

Figure 4.19: Stress strain curve of 84-day old samples

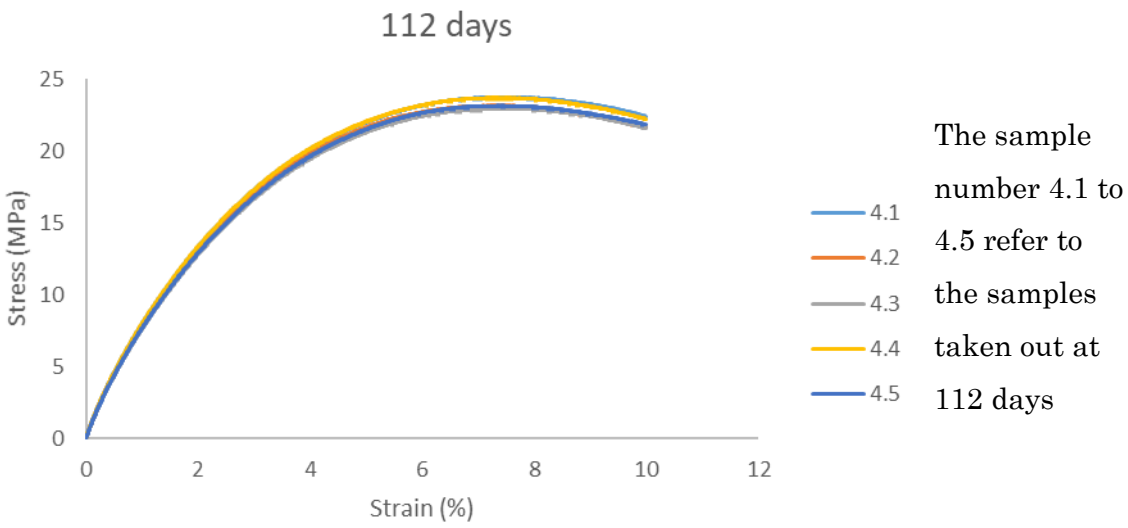

The sample number 4.1 to 4.5 refer to the samples taken out at 112 days

Figure 4.20: Stress strain curve of 112-day old samples

4.3.2 Flexural modulus

The flexural modulus is observed to increase gradually with a net increase of 4.6 % in 112 days. The increase with each age interval is smooth and doesn't involve any sharp changes.

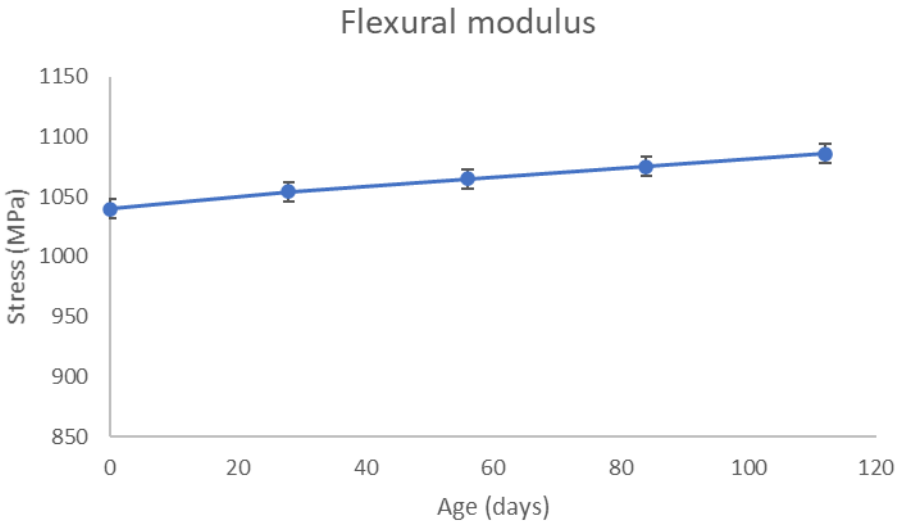

Figure 4.21: Flexural modulus vs age

4.3.3 Flexural strength

The flexural strength is also observed to increase very slightly, with a sharper increase from 28 to 54 days, followed by steady smoothing out up to 112 days, resulting in an overall increase of 2.39% The flexural strengths are higher than the tensile strengths, as during bending, the extreme regions of the HDPE are at stress, whereas with the tensile test, all the layers experience a stress causing it to have lower strength compared to bending(Ashby, 2011)

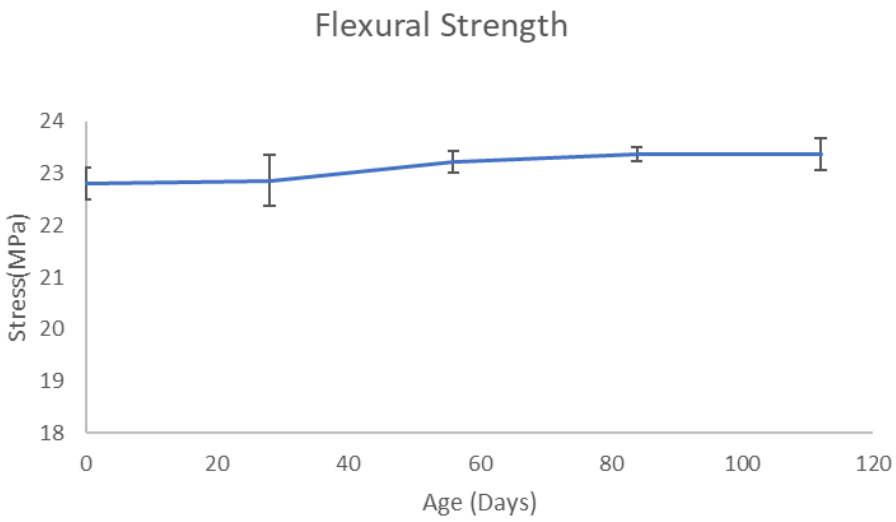

Figure 4.22: Flexural strength vs age

4.3.4 Overall flexural property change:

It is observed that aging does not affect the flexural properties by a large margin, with not more than a 5% increase compared to the value of the unaged specimens.

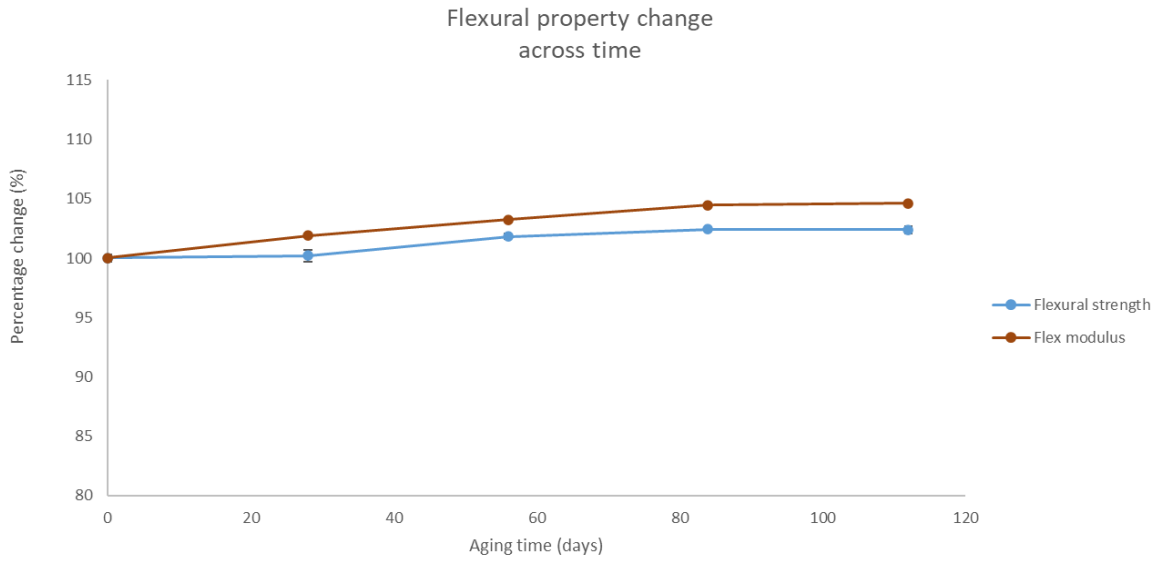

Figure 4.23: Flexural property change with age

4.4 Hyperspectral Imaging

Different surfaces reflect and absorb light in different ways. The reflectance property of a material depends on the type of material, chemical and physical state, surface roughness, angle of incident light etc. The reflectance also varies with the wavelength of the electromagnetic energy, therefore the amount of reflectance that can be measured as a function of wavelength is known as spectral reflectance. In this case, since all the graphs follow the same pattern, it is observed at around 600nm there exists the largest separation between the spectra. With spectral imaging, each spectrum that is analysed gives information more than just colour. Since all the samples were of the same colour(black), and there no significant changes in colour as seen with the naked eye, but the camera was able to pick up changes in brightness of the light reflected. The first 5 and the last 5 values of wavelength were omitted due to the noise leaked from the camera and hence followed as a standard procedure to obtain spectral values. The shape of the curves remains almost similar at each age interval, which represents a similar colour at a given wavelength, but a difference in the brightness of the light reflected at each age interval(Haaland et al., 2016).

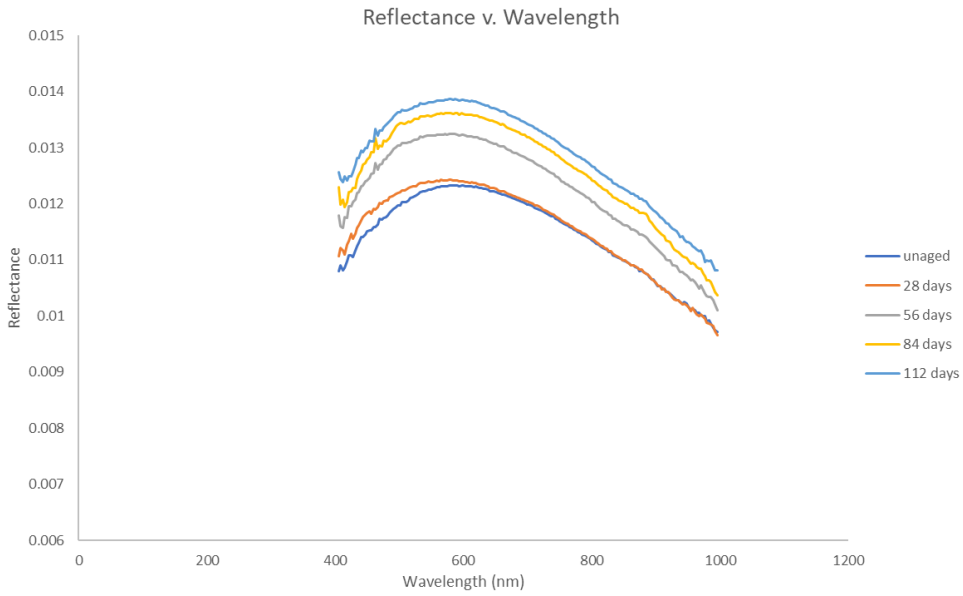

Figure 4.24: Spectral reflectance vs. wavelength

4.4.1 RMSE value of reflectance:

The Root mean square error is a metric that quantifies how different two spectra are by means of an error value. It is calculated by the formula below. It is square root of the average of squared errors. Thus, the effect of each error is proportional to the square of each error, thus larger the error, the larger effect on RMSE.

$$RMSE = \sqrt{\frac{1}{n}\sum_{i=1}^{n}(f_i - o_i)^2}$$

Where:

f_i – predicted value

o_i – actual value

n- number of values

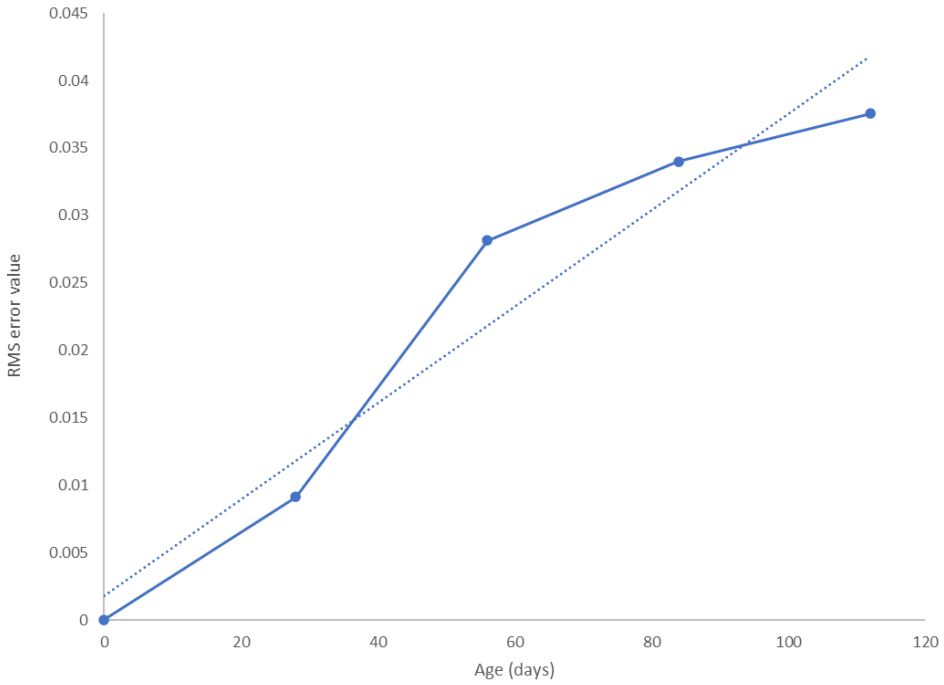

Figure 4.25: RMSE of reflectance vs time

From the above plot, it is observed that the difference in the reflectance is evident, with a slight change between 0 and 28 days followed by a jump at 56 days and a gradual increase up to 112 days.

4.4.2 Effect of aqueous medium on roughness of HDPE:

It is known that exposure to UV radiation increases the roughness of HDPE, up to the point of creating cracks on the surface, thereby greatly deteriorating the surface(Pucinelli et al., 2017). However, the aging conditions employed for this current study involves an aqueous stage, where the polymer is subjected to 12 hours of exposure to moisture along with 12 hours of UV exposure. A study by (G. et al., 2013) comments on the aging of a HDPE pipe that occurs in an aqueous environment. The pipes were suspended in distilled water and it was observed that by the end of the aging interval, the roughness of the inner surface had decreased by 4.9%. It was also found out that there was a gradual loss of hydrophobicity, with an observed weight loss across each aging interval. The loss of weight was attributed to degradation of material, with the surface smoothening out over time. The nature of the surface finish also plays an important role in how the roughness changes with aging.

This phenomenon, if true in the case of this study, could explain the increase in the reflectance picked up by the Hyperspectral imaging. The smoothening out of the surface, if present, would improve the reflectance of various wavelengths incident on the polymer surface.

4.4.3 Correlation between reflectance and mechanical properties:

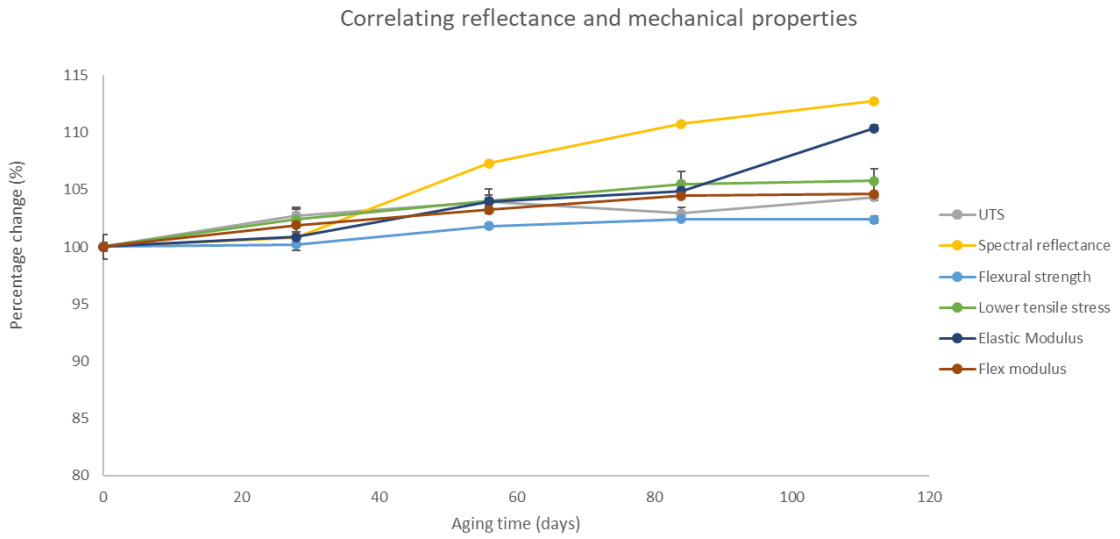

Figure 4.26: Plotting change in reflectance and mechanical properties

It is observed that the mechanical properties from both the tensile and flexural tests increases except for toughness and stress at break which decrease with time. The trend in reflectance can either be linked to one particular property that increases or all the properties that increase. This however cannot be concluded until further investigated over a longer period of time to see how the mechanical and hyperspectral properties change with time and to observe if all mechanical properties follow the same trend as the spectral reflectance or if it is one or few properties follow a similar trend. As it stands, up to 112 days there is a correlation in trend between the increase in spectral reflectance and the increase in the mechanical properties depicted in Fig 4.26.

5.Conclusion

Plastics are a low-cost material that offer marvellous material properties. HDPE has found its place in aquaculture due to its excellent strength, toughness, erosion resistance and inertness. HDPE, however, is subject to degradation as it is in contact with water, exposure to sunlight, fluctuations in temperature and cyclic temperature shocks due to freezing and thawing. These conditions greatly reduce the active lifetime of HDPE causing it to weaken over time, rendering it useless. The solution is to investigate the property degradation by various modes of testing and simulating scenarios of weathering to estimate the usable life of the HDPE by analysing the property degradation/change. After conducting the accelerated aging, mechanical testing and result computation, It can be concluded that the combined effect of aging has caused an increasing trend in most of the mechanical properties for an aging period of up to 112 days, as evident from the results and is confirmed from previous studies(Kiersnowska et al., 2020). However, prolonged aging causes degradation which was not visible with the current aging parameters and duration that was employed. Since the work is to be continued, this will be examined at a later stage. Another interesting finding is that HSI can pick up an increasing trend in spectral reflectance values, which is analogous to the increasing trend in some of the mechanical properties.

6. Future Work

1. Since HSI is a surface level technique, it does not penetrate beyond the surface level. In order to obtain a better correlation of the spectral data to degradation, the samples are to be polished in stages to analyse each layer and also to get a better understanding of how deep in the material the properties can be mapped.
2. The samples would undergo FTIR analysis to analyse the chemical changes that occur due to the aging and, to better understand the reason for the change in mechanical properties, loss in weight etc.
3. The UV and the moisture based aging phases would be separated on the aging chambers and exposed to the elements individually. This is done to get a better understanding of how these elements affect the polymer, as in the current study, the combined effect of aging is studied and it is hard to decipher which cycle is responsible for certain observed phenomena. i.e.: decreasing roughness with age.
4. It is hypothesised that roughness decreases with age, hence, to get a better understanding of the surface changes, the samples would be analysed using a profilometer or atomic force microscope.
5. The samples aged up to 224 days are to be tested to fulfil the L'banks aging criteria to get a better understanding of the polymer degradation with time. This would serve as a good database for better estimation of HDPE degradation and for lifetime prediction.
6. Trying to obtain a deeper correlation and understanding of how the spectral properties and mechanical properties can be correlated and to arrive at a damage index that would serve as a connecting link between them.

7.References

ABDELKADER, D., MOSTEFA, B., ABDELKRIM, A., ABDERRAHIM, T., NOUREDDINE, B. & MOHAMED, B. 2015. Fatigue Life Prediction and Damage Modelling of High-density Polyethylene under Constant and Two-block Loading. *Procedia Engineering,* 101**,** 2-9.

AKVAGROUP. 2018. *Cage Farming* [Online]. Available: https://www.akvagroup.com/pen-based-aquaculture/pens-nets/plastic-pens [Accessed].

AMJADI, M. & FATEMI, A. 2020. Tensile Behavior of High-Density Polyethylene Including the Effects of Processing Technique, Thickness, Temperature, and Strain Rate. *Polymers,* 12**,** 1857.

ANDRADY, A. L. 2011. Microplastics in the marine environment. *Marine Pollution Bulletin,* 62**,** 1596-1605.

ASC 2018. ASC joins fight against marine plastics.

ASHBY, M. F. 2011. Chapter 5 - Materials Selection—The Basics. *In:* ASHBY, M. F. (ed.) *Materials Selection in Mechanical Design (Fourth Edition).* Oxford: Butterworth-Heinemann.

BANK, L. C., GENTRY, T. R., THOMPSON, B. P. & RUSSELL, J. S. 2003. A model specification for FRP composites for civil engineering structures. *Construction and Building Materials,* 17**,** 405-437.

BARAN, J., JANIK, A., RYSZKO, A. & SZAFRANIEC, M. Towards a circular economy in Poland: are we moving to a recycling society. Carpathian Logistics Congress, 2016. 463-469.

BECERRA, A. F. C. & D'ALMEIDA, J. R. M. 2017. UV Effects on the Tensile and Creep Behaviour of HDPE. *Polymers and Polymer Composites,* 25**,** 327-332.

BHUYAR, P., TAMIZI, N., AB. RAHIM, M. H., MANIAM, G. P. & GOVINDAN, N. 2019. Effect of ultraviolet light on the degradation of Low-Density and High-Density Polyethylene characterized by the weight loss and FTIR. 1**,** 26-31.

BRINGER, A., THOMAS, H., PRUNIER, G., DUBILLOT, E., BOSSUT, N., CHURLAUD, C., CLÉRANDEAU, C., LE BIHANIC, F. & CACHOT, J. 2020. High density polyethylene (HDPE) microplastics impair development and swimming activity of Pacific oyster D-larvae, Crassostrea gigas, depending on particle size. *Environmental Pollution,* 260**,** 113978.

CALLISTER, W. D. 2007. *Materials Science and Engineering: An Introduction*, John Wiley & Sons, Incorporated.

CALVINI, R., AMIGO, J. M. & ULRICI, A. 2017. Transferring results from NIR-hyperspectral to NIR-multispectral imaging systems: A filter-based simulation applied to the classification of Arabica and Robusta green coffee. *Analytica chimica acta,* 967**,** 33-41.

CERESANA. 2019. *Polyethylene - HDPE Market Report* [Online]. Available: https://www.ceresana.com/en/market-studies/plastics/polyethylene-hdpe/ [Accessed 2020].

CHANG, C. I. 2003. *Hyperspectral Imaging: Techniques for Spectral Detection and Classification*, Springer US.

CHARTER, M. 2018. *Designing for the Circular Economy*, Taylor & Francis.

CHEMTEC 2015. 7 - UV DEGRADATION & STABILIZATION OF POLYMERS & RUBBERS. *In:* WYPYCH, G. (ed.) *Handbook of UV Degradation and Stabilization (Second Edition).* ChemTec Publishing.

CLIMATE, W. 2019. *Weather conditions in Hjemeland* [Online]. Available: https://weather-and-climate.com/average-monthly-precipitation-Rainfall,hjelmeland-rogaland-no,Norway [Accessed].

COLE, M., LINDEQUE, P., HALSBAND, C. & GALLOWAY, T. S. 2011. Microplastics as contaminants in the marine environment: A review. *Marine Pollution Bulletin,* 62**,** 2588-2597.

CRAIG, I. H., WHITE, J. R., SHYICHUK, A. V. & SYROTYNSKA, I. 2005. Photo-induced scission and crosslinking in LDPE, LLDPE, and HDPE. *Polymer Engineering & Science,* 45**,** 579-587.

CYSNE BARBOSA, A. P., P. FULCO, A. P., S.S. GUERRA, E., K. ARAKAKI, F., TOSATTO, M., B. COSTA, M. C. & D. MELO, J. D. 2017. Accelerated aging effects on carbon fiber/epoxy composites. *Composites Part B: Engineering,* 110**,** 298-306.

DEMIRBAY, B. 2017. *Film formation, morphological, optical and electrical percolation behaviors of PS/MWCNT and PS/GO nanocomposite films.*

DEVASAHAYAM, S., BHASKAR RAJU, G. & MUSTANSAR HUSSAIN, C. 2019. Utilization and recycling of end of life plastics for sustainable and clean industrial processes including the iron and steel industry. *Materials Science for Energy Technologies,* 2**,** 634-646.

DHINESH, S. K., ARUN, P. S., SENTHIL, K. K. L. & MEGALINGAM, A. 2020. Study on flexural and tensile behavior of PLA, ABS and PLA-ABS materials. *Materials Today: Proceedings*.

DUPUIS, A., PERRIN, F.-X., TORRES, A. U., HABAS, J.-P., BELEC, L. & CHAILAN, J.-F. 2017. Photo-oxidative degradation behavior of linseed oil based epoxy resin. *Polymer Degradation and Stability,* 135**,** 73-84.

DYREVERNALLIANSEN. 2016. *Fish farming in Norway* [Online]. Available: https://www.dyrevern.no/english/fish-farming-in-norway [Accessed].

ELMASRY, G. & SUN, D.-W. 2010. CHAPTER 1 - Principles of Hyperspectral Imaging Technology. *In:* SUN, D.-W. (ed.) *Hyperspectral Imaging for Food Quality Analysis and Control.* San Diego: Academic Press.

EYERER, P. 2010. Plastics: Classification, Characterization, and Economic.

FENG, Z., ZHANG, T., LI, Y., HE, X., WANG, R., XU, J. & GAO, G. 2019. The accumulation of microplastics in fish from an important fish farm and mariculture area, Haizhou Bay, China. *Science of The Total Environment,* 696**,** 133948.

FRIAS, J. P. G. L. & NASH, R. 2019. Microplastics: Finding a consensus on the definition. *Marine Pollution Bulletin,* 138**,** 145-147.

G., W., HABECHE, C., K., HAOUI, A., Z. & ZARI. Surface Degradation and Crystallinity Changes in HDPE-100 Pipe Subjected to Chemical Aggressive Environments. 2013.

GRIGORIADOU, I., PARASKEVOPOULOS, K. M., CHRISSAFIS, K., PAVLIDOU, E., STAMKOPOULOS, T. G. & BIKIARIS, D. 2011. Effect of different nanoparticles on HDPE UV stability. *Polymer Degradation and Stability,* 96**,** 151-163.

GULMINE, J. V. & AKCELRUD, L. 2006. Correlations between structure and accelerated artificial ageing of XLPE. *European Polymer Journal,* 42**,** 553-562.

GULMINE, J. V., JANISSEK, P. R., HEISE, H. M. & AKCELRUD, L. 2003. Degradation profile of polyethylene after artificial accelerated weathering. *Polymer Degradation and Stability,* 79**,** 385-397.

HAALAND, D. M., JONES, H. D. T. & TIMLIN, J. A. 2016. Chapter 12 - Experimental and Data Analytical Approaches to Automating Multivariate Curve Resolution in the Analysis of Hyperspectral Images. *In:* RUCKEBUSCH, C. (ed.) *Data Handling in Science and Technology.* Elsevier.

HE, H.-J., WU, D. & SUN, D.-W. 2013. Non-destructive and rapid analysis of moisture distribution in farmed Atlantic salmon (Salmo salar) fillets using visible and near-infrared hyperspectral imaging. *Innovative Food Science & Emerging Technologies,* 18**,** 237-245.

HSUEH, H.-C., KIM, J. H., ORSKI, S., FAIRBROTHER, A., JACOBS, D., PERRY, L., HUNSTON, D., WHITE, C. & SUNG, L. 2020. Micro and macroscopic mechanical behaviors of high-density polyethylene under UV irradiation and temperature. *Polymer Degradation and Stability,* 174**,** 109098.

INSTRON 2016. Tensile standards.

IUCN. 2018. *Marine Plastics* [Online]. Available: https://www.iucn.org/resources/issues-briefs/marine-plastics [Accessed 20/3 2020].

KAYNAK, C. & SARı, B. 2016. Accelerated weathering performance of polylactide and its montmorillonite nanocomposite. *Applied Clay Science,* 121-122**,** 86-94.

KETOLA, W. D., GROSSMAN, D., MATERIALS, A. C. G.-O. D. O. N. & TESTS, A. S. D. O. A. 1994. *Accelerated and Outdoor Durability Testing of Organic Materials*, ASTM.

KIERSNOWSKA, A., FABIANOWSKI, W. & KODA, E. 2020. The Influence of the Accelerated Aging Conditions on the Properties of Polyolefin Geogrids Used for Landfill Slope Reinforcement. *Polymers,* 12**,** 1874.

KOKKA, A., PULLI, T., HONKAVAARA, E., MARKELIN, L., KÄRHÄ, P. & IKONEN, E. 2019. Flat-field calibration method for hyperspectral frame cameras. *Metrologia,* 56**,** 055001.

KUTZ, M. 2017. Preface to the Second Edition. *In:* KUTZ, M. (ed.) *Applied Plastics Engineering Handbook (Second Edition).* William Andrew Publishing.

LU, T., SOLIS-RAMOS, E., YI, Y. & KUMOSA, M. 2018. UV degradation model for polymers and polymer matrix composites. *Polymer Degradation and Stability,* 154**,** 203-210.

MATHIEU, E. & LAURENT, J.-L. 1996. Comparison of two instruments for accelerated weathering tests on plasticized PVC. *Polymer Degradation and Stability,* 51**,** 77-81.

MECHANICALC 2013. Mechanical Properties of Materials.

NICHOLSON, L., WHITLEY, K., GATES, T. & HINKLEY, J. 2000. How Molecular Structure Affects Mechanical Properties Of An Advanced Polymer.

NIEMSAKUL, S., SAE-EAWA, N. & AUE-U-LAN, Y. 2018. Determination and analysis of critical damage criteria for predicting fracture in forming process by uniaxial tensile test. *Materials Today: Proceedings,* 5**,** 9642-9650.

OJHA, S. N. & BABU, S. C. 2019. Chapter 17 - Why convergence of Fisheries Co-management with Agricultural Technology Management Agency is significant. *In:* BABU, S. C. & JOSHI, P. K. (eds.) *Agricultural Extension Reforms in South Asia.* Academic Press.

PE100 2016. Environmental position of HDPE Pipes.

PEACOCK, A. 2000. *Handbook of Polyethylene: Structures: Properties, and Applications*, CRC Press.

PETERLIN, A. 1967. Plastic deformation of polyethylene. Mechanism and properties. *Journal of Polymer Science Part C: Polymer Symposia,* 15**,** 427-443.

PLASTICSEUROPE 2016. Thermoplastics.

PLATZER, N. 1986. Encyclopedia of Polymer Science and Engineering, H. F. Mark, N. M. Bikales, C. G. Overberger, and G. Menges, Wiley-Interscience, New York, 1985, 720 pp. *Journal of Polymer Science Part C: Polymer Letters,* 24**,** 359-360.

POLANCO-LORIA, M., CLAUSEN, A., BERSTAD, T. & HOPPERSTAD, O. 2010. Constitutive model for thermoplastics with structural applications. *International Journal of Impact Engineering,* 37**,** 1207-1219.

PUCINELLI, C., SILVA, R., MELLARA, T., GATON, P., PIRES-DE-SOUZA, F. & SILVA, L. 2017. Color Stability and Surface Roughness of Composites after Artificial Accelerated Aging. *Journal of Dentistry Indonesia,* 24.

QIAO, M., QIANPING, R., WU, S. & SHEN, J. 2009. Impact of ultraviolet radiation on HDPE and HDPE/STC blends. *Polymers for Advanced Technologies - POLYM ADVAN TECHNOL,* 20**,** 341-346.

QLAB 2017. QUV - The World's Most Widely Used Weathering Tester.

RAM, A. 1997. The Chemistry of Polymers. *In:* RAM, A. (ed.) *Fundamentals of Polymer Engineering.* Boston, MA: Springer US.

ROESLER, J., HARDERS, H. & BAEKER, M. 2007. *Mechanical Behaviour of Engineering Materials: Metals, Ceramics, Polymers, and Composites*, Springer Berlin Heidelberg.

RÖSLER, J., HARDERS, H. & BAEKER, M. 2007. *Mechanical Behaviour of Engineering Materials: Metals, Ceramics, Polymers, and Composites*.

SAHU, A. K. & SUDHAKAR, K. 2019. Effect of UV exposure on bimodal HDPE floats for floating solar application. *Journal of Materials Research and Technology,* 8**,** 147-156.

SALIH, S., HAMOOD, A. A. & ABD ALSALAM, A. 2013. Comparison of the characteristics of LDPE: PP and HDPE: PP polymer blends. *Modern Applied Science,* 7**,** 33-42.

SCHNEIDER, A. & FEUSSNER, H. 2017. Chapter 5 - Diagnostic Procedures. *In:* SCHNEIDER, A. & FEUSSNER, H. (eds.) *Biomedical Engineering in Gastrointestinal Surgery.* Academic Press.

SCOTT, G. 1999. *Polymers and the Environment*, Royal Society of Chemistry.

SENDIN, K., WILLIAMS, P. J. & MANLEY, M. 2018. Near infrared hyperspectral imaging in quality and safety evaluation of cereals. *Critical reviews in food science and nutrition,* 58**,** 575-590.
SHEBANI, A., KLASH, A., ELHABISHI, R. G., ABDSALAM, S., ELBREKI, H. & ELHRARI, W. K. The Influence of LDPE Content on the MechanicalProperties of HDPE/LDPE Blends. 2018.
SHRIVASTAVA, A. 2018. 3 - Plastic Properties and Testing. *In:* SHRIVASTAVA, A. (ed.) *Introduction to Plastics Engineering.* William Andrew Publishing.
SKAULI, T. 2012. An upper-bound metric for characterizing spectral and spatial coregistration errors in spectral imaging. *Opt Express,* 20**,** 918-33.
SKAULI, T., HAAVARDSHOLM, T., KÅSEN, I., OPSAHL, T., KAVARA, A. & SKAUGEN, A. Hyperspectral Imaging Technology and Systems, Exemplified by Airborne Real-time Target Detection. CLEO:2011 - Laser Applications to Photonic Applications, 2011/05/01 2011 Baltimore, Maryland. Optical Society of America, CMG5.
SZABO, T. L. 2005. Chapter 10 - Degradation and environmental effects. *In:* SZABO, T. L. (ed.) *Plastics (Third Edition).* Oxford: Butterworth-Heinemann.
TANYILDIZI, H. 2018. Long-term microstructure and mechanical properties of polymer-phosphazene concrete exposed to freeze-thaw. *Construction and Building Materials,* 187**,** 1121-1129.
TIDWELL, J. H. & BRIGHT, L. A. 2019. Freshwater Aquaculture. *In:* FATH, B. (ed.) *Encyclopedia of Ecology (Second Edition).* Oxford: Elsevier.
TORIKAI, A., CHIGITA, K. I., OKISAKI, F. & NAGATA, M. 1995. Photooxidative degradation of polyethylene containing flame retardants by monochromatic light. *Journal of applied polymer science,* 58**,** 685-690.
VAN CAUWENBERGHE, L., DEVRIESE, L., GALGANI, F., ROBBENS, J. & JANSSEN, C. R. 2015. Microplastics in sediments: A review of techniques, occurrence and effects. *Marine Environmental Research,* 111**,** 5-17.
VERT, M., DOI, Y., HELLWICH, K.-H., HESS, M., HODGE, P., KUBISA, P., RINAUDO, M. & SCHUÉ, F. 2012. Terminology for biorelated polymers and applications (IUPAC Recommendations 2012). *Pure and Applied Chemistry.*
XU, M. M., HUANG, G. Y., FENG, S. S., MCSHANE, G. J. & STRONGE, W. J. 2016. Static and Dynamic Properties of Semi-Crystalline Polyethylene. *Polymers (Basel),* 8.
YANG, T.-C., NOGUCHI, T., ISSHIKI, M. & WU, J.-H. 2014. Effect of titanium dioxide on chemical and molecular changes in PVC sidings during QUV accelerated weathering. *Polymer Degradation and Stability,* 104**,** 33-39.

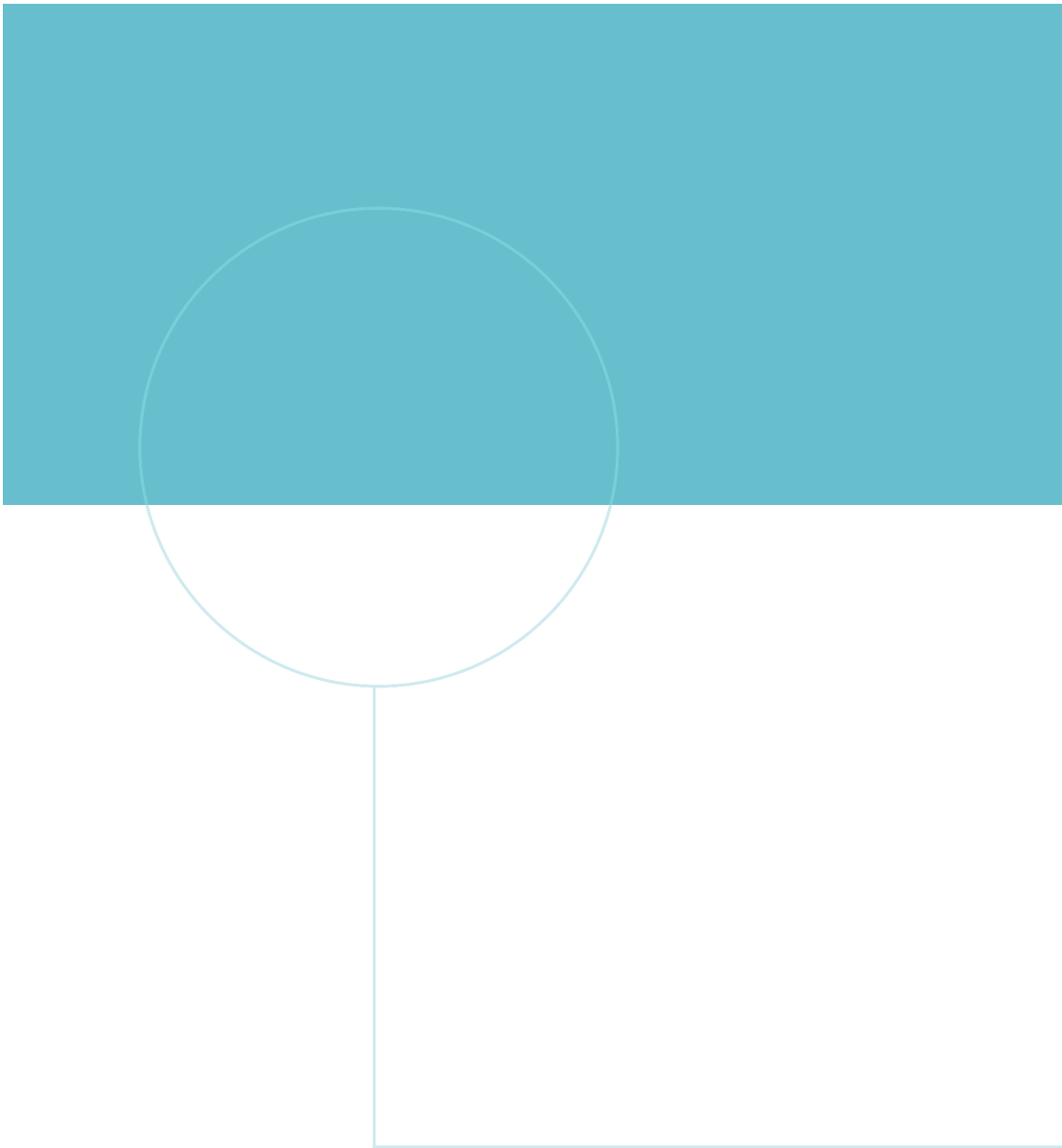

NTNU

Norwegian University of
Science and Technology